ARPA ORDER.: 3520
9K10 Director's Office

-1014-ARPA

ebruary 1979

OPAGATION OF Lg SEISMIC WAVES IN THE SOVIET UNION

rles Shishkevish

A Rand Note
prepared for the
DEFENSE ADVANCED RESEARCH PROJECTS AGENCY

Rand
SANTA MONICA, CA. 90406

The research described in this report was sponsored by the Defense Advanced Research Projects Agency under Contract No. MDA903-78-C-0189.

Published by The Rand Corporation

UNCLASSIFIED

SECURITY CLASSIFICATION OF THIS PAGE (When Data Entered)

AD A072844

REPORT DOCUMENTATION PAGE

READ INSTRUCTIONS BEFORE COMPLETING FORM

1. REPORT NUMBER: (14) RAND/N-1014-ARPA	2. GOVT ACCESSION NO.
3. RECIPIENT'S CATALOG NUMBER	
4. TITLE (and Subtitle): (6) Propagation of Lg Seismic Waves in the Soviet Union	5. TYPE OF REPORT & PERIOD COVERED: (9) Interim rept.
6. PERFORMING ORG. REPORT NUMBER	
7. AUTHOR(s): (10) Charles Shishkevish	8. CONTRACT OR GRANT NUMBER(s): (15) MDA903-78-C-0189, ARPA Order-3500
9. PERFORMING ORGANIZATION NAME AND ADDRESS: The Rand Corporation, 1700 Main Street, Santa Monica, California 90406	10. PROGRAM ELEMENT, PROJECT, TASK AREA & WORK UNIT NUMBERS
11. CONTROLLING OFFICE NAME AND ADDRESS: Defense Advanced Research Projects Agency, Department of Defense, Arlington, Virginia 22209	12. REPORT DATE: (11) Feb[illegible]1979; NUMBER OF PAGES: 62
14. MONITORING AGENCY NAME & ADDRESS (if different from Controlling Office): (12) 76p.	15. SECURITY CLASS. (of this report): Unclassified; 15a. DECLASSIFICATION/DOWNGRADING SCHEDULE

16. DISTRIBUTION STATEMENT (of this Report)

Approved for Public Release; Distribution Unlimited

17. DISTRIBUTION STATEMENT (of the abstract entered in Block 20, if different from Report)

No Restrictions

18. SUPPLEMENTARY NOTES

FILE COPY

19. KEY WORDS (Continue on reverse side if necessary and identify by block number)

Seismic Detection
Nuclear Explosion Detection
Shock Waves
Geology
Earthquakes
Wave Propagation

20. ABSTRACT (Continue on reverse side if necessary and identify by block number)

DDC

See Reverse Side

296 600 Gu

DD FORM 1 JAN 73 1473 EDITION OF 1 NOV 65 IS OBSOLETE

UNCLASSIFIED

SECURITY CLASSIFICATION OF THIS PAGE (When Data Entered)

this report

Summarizes the data on the Lg phase, a seismic wave-train with periods between 0.5 and 6 sec transmitted in the continental crust with a group velocity of 3.44 to 3.57 km/sec, propagating in the Soviet Union and nearby areas. Amplitude-distance curves and amplitude-distance correction factor data used in determining the magnitudes of Lg are given. The available travel time data, including the "standard" travel times of Lg, are summarized. Analysis of the efficiency of propagation of Lg by Soviet seismologists shows that Lg propagates efficiently across the Indian shield, Tarim basin, and the Russian, Siberian, and Kazakh platforms. It propagates less efficiently along Tien Shan and the Himalayas. The Tibetan platform, central part of the Black Sea, and central and eastern parts of the Caspian Sea completely eliminate Lg. 62 pp. 4 Ref. (Author)

ARPA ORDER.: 3520
9K10 Director's Office

N-1014-ARPA

February 1979

PROPAGATION OF Lg SEISMIC WAVES IN THE SOVIET UNION

Charles Shishkevish

A Rand Note

prepared for the

DEFENSE ADVANCED RESEARCH PROJECTS AGENCY

Rand
SANTA MONICA, CA. 90406

PREFACE

This Rand Note is part of a continuing Rand study of selected areas of Soviet science and technology, a project sponsored by the Defense Advanced Research Projects Agency. It is the first in a series of at least three studies requested by the Nuclear Monitoring Research Office of DARPA in support of their research on seismic detection and discrimination of underground nuclear explosions at regional distances (less than 2000 km). The present note describes the characteristics of the Lg phase, a seismic wavetrain with periods between 0.5 and 6 s transmitted in the continental crust with a group velocity between 3.44 and 3.57 km/s, propagating in the Soviet Union and nearby regions. The second and third reports in this series, on the characteristics of Rg and Pn in the Soviet Union, are scheduled for publication later this year. If sufficient useful data are available on other crustal and upper mantle phases such as Pg, Sn, etc. propagating in the Soviet Union, these phases may also be covered in future reports. The present note is an extensive summary of pertinent Soviet research on Lg that is intended for U.S. seismologists developing regional discriminants for the detection and identification of underground nuclear explosions. It is also intended for seismologists and geologists dealing with the interpretation of seismic data acquired at regional distances. Time permitting, this and future reports on Rg, Pn and other phases will be combined into a single report summarizing and critically analyzing the Soviet research on the characteristics of these phases propagating in the Soviet Union. The author welcomes any comments, suggestions and criticisms. All correspondence should be sent to The Rand Corporation, 2100 M Street, N.W., Washington, D.C., 20037.

INTRODUCTION AND SUMMARY

The Lg phase is a seismic wavetrain with periods ranging from 0.5 to 6 s, propagating with a group velocity between 3.44 and 3.57 km/s, the velocity of shear waves in the crust. One of the most characteristic properties of the Lg is that it is not transmitted across deep ocean basins. The efficiency of propagation of Lg across continental paths also varies greatly. Propagation of Lg is most efficient across stable shield and platform regions with a relatively homogeneous, high-Q crust, where Lg is the predominant phase recorded at Δ = 250 to 4000 km and where it is frequently observed at epicentral distances to 6000 km. It propagates less efficiently in certain large mountain-range regions with abnormally thick crust, especially along paths parallel to these ranges. The Lg does not propagate across all or parts of marginal and inland seas with non-continental crust characterized by the absence of the granitic layer. It has therefore been suggested that the efficiency of propagation of Lg depends on the presence as well as the thickness of the granitic layer; that propagation is very efficient when the thickness is normal, less efficient when it is thin and zero (no Lg) when it is absent.

The Lg phase forms a distinct wavetrain with sharp, steep onsets and amplitudes larger than other conventional phases. Thus, the amplitudes of Lg are usually from 5 to 50 times greater than the peak amplitudes of P. The duration of Lg recorded at a few hundred kilometers is 20 to 30 s, increasing with distance and reaching 60 to 90 s at Δ = 2000 to 3000 km.

Analysis of Lg confirms the presence of two phases: Lg_1 and Lg_2. The Lg_1 phase propagating with a velocity of 3.51 to 3.62 km/s is recorded as a first arrival at epicentral distances up to 1500 km. At longer distances, the Lg_1 is replaced by Lg_2 propagating with a velocity of 3.28 to 3.41 km/s and having slightly longer periods. Both Lg_1 and Lg_2 are frequently observed together throughout the whole range of distances over which they are recorded. Another phase, the Lg_i with a velocity of 3.7 to 3.8 km, is sometimes recorded by

intermediate-period seismographs. However, its amplitudes are much smaller and the Lg_i is frequently not recorded even when Lg is the predominant phase on the seismogram. The Lg phase, with periods varying between 0.5 s at the beginning of the seismogram and 2.5 s at its end, is clearly recorded by short-period instruments. The Lg recorded with intermediate-period seismographs has periods that increase with distance, reaching 5 to 7 s at Δ = 3000 to 4000 km. The periods of Lg also increase with increasing magnitude of earthquakes. The motion of Lg is mostly horizontal, although the vertical and radial components are also strong. The Lg phase is characterized by the absence of dispersion.

The early Soviet work on Lg dealt mostly with the determination of the general characteristics of Lg recorded at a few Soviet seismographic stations, i.e., the group velocity of Lg_1 and Lg_2, their period ranges and gross features of the propagation efficiency of Lg [15-20]. The first very extensive analysis of Lg and other phases was published by Nersesov and Rautian [1]. It was based on data from 37 earthquakes acquired during 1961-1962 by short-period, three-component SKM-3 seismographs at 54 temporary seismographic stations set up along a 3500-km-long profile, extending between the Pamir Mountains and Lena River (profile A-A' in Fig. 1a). The authors plotted the amplitude-distance curves of various phases including Lg from earthquakes originating in three different regions in the Soviet Union, recorded at epicentral distance ranges between a few hundred and 3000 km. They also tabulated the travel times of Lg for the south-southeastern part of the Soviet Union.

In a 1971 paper [2], Antonova determined the amplitude-distance curves of several phases, including Lg, from 40 crustal earthquakes with K = 9.7 to 14, recorded with three-component, short-period SKM-3 seismograph systems operating at 12 seismographic stations in North Tien Shan located in the vicinity of Lake Issyk Kul, 11 of which are shown in Fig. 1b. The mean spectral amplitude-distance curves of Lg from 170 earthquakes, acquired with the seven-channel, vertical component ChISS seismograph at the Talgar station (7 in Fig. 1a, 11 in Fig. 1b) were determined and published in a paper by Nurmagambetov [5].

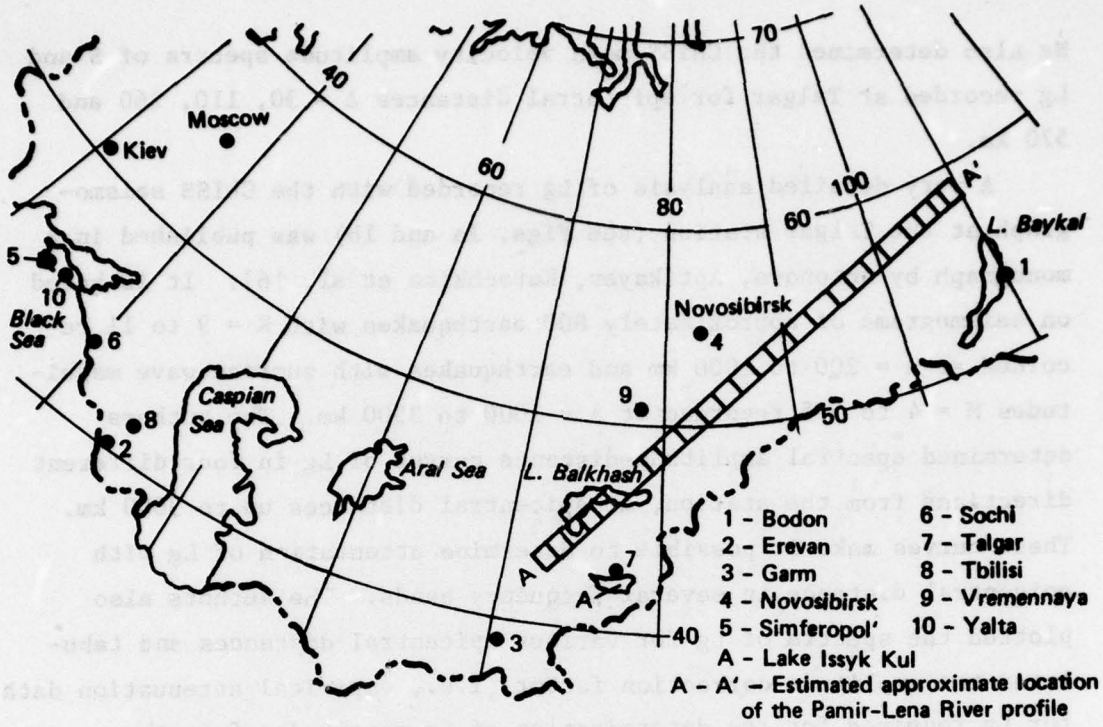

Fig. 1a — Locations of seismographic stations and the Pamir-Lena River profile, the data from which are used in this note

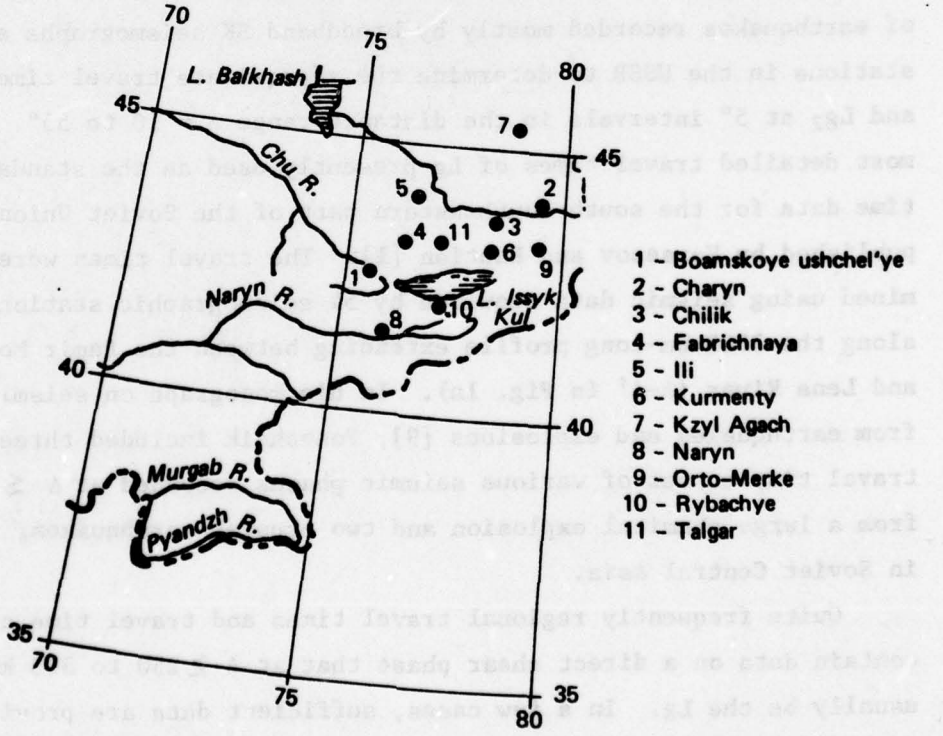

Fig. 1b — Locations of North Tien Shan seismographic stations, the data from which are used in this note

He also determined the ChISS mean velocity amplitude spectra of S and Lg recorded at Talgar for epicentral distances Δ = 30, 110, 260 and 570 km.

A very detailed analysis of Lg recorded with the ChISS seismograph at the Talgar station (see Figs. 1a and 1b) was published in a monograph by Antonova, Aptikayev, Kurochkina et al. [6]. It is based on seismograms of approximately 800 earthquakes with K = 9 to 11 recorded at Δ = 200 to 1000 km and earthquakes with surface wave magnitudes M = 4 to 5.5 recorded at Δ = 1000 to 3500 km. The authors determined spectral amplitude-distance curves of Lg in four different directions from the station, at epicentral distances up to 3000 km. These curves make it possible to determine attenuation of Lg with epicentral distance in several frequency bands. The authors also plotted the spectra of Lg for various epicentral distances and tabulated the amplitude correction factor, i.e., empirical attenuation data for Lg required for the determination of Lg magnitudes from the Gutenberg-Richter formula.

In a paper published in 1961 [12] Vald'ner used 120 seismograms of earthquakes recorded mostly by broadband SK seismographs at base stations in the USSR to determine the approximate travel times of Lg_1 and Lg_2 at 5° intervals in the distance range Δ = 10 to 55°. The most detailed travel times of Lg presently used as the standard travel time data for the south-southeastern part of the Soviet Union were published by Nersesov and Rautian [1]. The travel times were determined using seismic data acquired by 54 seismographic stations located along the 3500-km-long profile extending between the Pamir Mountains and Lena River (A-A' in Fig. 1a). In his monograph on seismic waves from earthquakes and explosions [9], Pasechnik included three sets of travel time curves of various seismic phases recorded at $\Delta \lesssim 1200$ km, from a large chemical explosion and two crustal earthquakes, originating in Soviet Central Asia.

Quite frequently regional travel times and travel time curves contain data on a direct shear phase that at $\Delta \geq 250$ to 300 km should usually be the Lg. In a few cases, sufficient data are provided to definitely identify this wave group as being the Lg phase. Thus, the

regional travel times of various body waves at $\Delta \leq 600$ km, propagating along the Chatkal range-Chuy-Ili valleys profile in Kirgizia (see Fig. 15) determined by Medzhitova and Sabitova [13] from seismograms of 26 earthquakes recorded by 21 seismographic stations include the times of Lg at 10 km intervals at epicentral distances Δ = 210 to 600 km. These data are in good agreement with the standard Lg times by Nersesov and Rautian. In a similar fashion, the travel time curves of body waves plotted by Tsibul'chik [14] for the Altay-Sayan and Tuva regions in Siberia using seismic data acquired by temporary and permanent stations in this area contain a curve for Lg at $\Delta \simeq$ 300 to 1100 km.

The differences in crustal structure of various regions of the Soviet Union determined on the basis of the efficiency of propagation of Lg and Rg across these regions were investigated in [6,8,11,15,25]. The data from several hundred earthquakes recorded by numerous seismographic stations indicate the absence of Lg along paths traversing the central part of the Black Sea [11,18-22]. Similar analysis performed in [18,19] also indicates that Lg and Rg are absent from seismograms when their paths traverse the central and eastern parts of the Caspian Sea.

The propagation of Lg across a large area in Central Asia, between 75° and 125° E Long. and 20 and 55° N Lat., was investigated in [6,8,23,24]. The analysis was based on several hundred seismograms of earthquakes acquired by a group of Soviet stations north of this area (Talgar, Novosibirsk, Bodon, Garm), plotted in Fig. 1a, equipped with multiple-bandpass ChISS seismographs and a group of WWSSN stations south of the area (in India and southeastern Asia) equipped with standard, short-period and intermediate-band seismographs. The efficiency of propagation of Lg was investigated by examining the seismograms to see if Lg is strong, weak, or absent. It was determined that Lg propagates efficiently across the Indian shield, Tarim basin and the Russian, Siberian and Kazakh platforms. It propagates less efficiently across Tien Shan and Hindu Kush and much less efficiently along Tien Shan and especially along the Himalayas. The Tibetan plateau forms an insurmountable barrier to Lg and even 100 to 150 km of the path along Tibet is sufficient to completely eliminate Lg.

The efficiency of propagation of Lg across Central Asia and adjacent regions was also investigated in [25] using records from as many as 54 seismographic stations along the Pamir-Lena River profile (A-A' in Fig. 1a). Analysis of a small number of earthquakes indicates that the amplitudes of Lg decrease 3 to 7 times across Altay, 6 to 8 times across the Himalayas and 10 times across Tibet.

SYMBOLS

A - amplitude of a seismic wave on the seismogram

D_g - galvanometer damping factor (fraction of critical damping)

D_s - seismometer damping factor (fraction of critical damping)

f - frequency of a seismic wave

k - a constant

K - energy class of an earthquake, $K = \log_{10}E$, where E is the energy of the earthquake in Joules

Lg - seismic wavetrain with a period between 0.5 and 6 s transmitted in the continental crust with a group velocity between 3.44 and 3.57 km/s

Lg_1 - Lg phase with a group velocity of 3.51 to 3.62 km/s

Lg_2 - Lg phase with a group velocity of 3.28 to 3.41 km/s

Lg_i - Lg phase with a group velocity of 3.7 to 3.8 km/s

M(M_s) - surface-wave magnitude of an earthquake or explosion. The subscript when given identifies the phase.

m(m_b) - body-wave magnitude of an earthquake or explosion. The subscript when given identifies the phase.

-N - the slope of the amplitude-distance curve plotted on a log-log scale

P - compressional body waves

$\overline{P}$(Pg) - direct compressional wave propagating in the granitic layer

P^*(Pb) - compressional wave along the Conrad discontinuity (top of the basaltic layer)

Pn - compressional wave along the Mohorovicic discontinuity (top of the upper mantle)

Q - specific quality factor

Q_M - amplitude-distance correction factor, i.e., an empirical attenuation curve

r - distance in km or degrees

Rg - a short period surface (Rayleigh) wave

S - shear body waves

$\overline{S}$(Sg) - direct shear wave propagating in the granitic layer

S^*(Sb) - shear wave along the Conrad discontinuity (top of the basaltic layer)

Sn - shear wave along the Mohorovicic discontinuity (top of the upper mantle)

T - period of the seismic wave

T_g - galvanometer period

V_s - group velocity of a seismic wave

β_K - function in the expression for the variation of the amplitude of a seismic wave on the seismogram with the energy class K, that decreases monotonically with frequency

β_M - function in the expression for the variation of the amplitude of a seismic wave on the seismogram with the surface wave magnitude M, that decreases monotonically with frequency.

γ - coefficient of inelastic attenuation, $\gamma = \Pi/V_g TQ$

$\gamma\ (f_i/f_j)$ - the logarithm of the ratio of spectral amplitude of Lg at frequencies f_i and f_j

Δ - epicentral distance in km or degrees

Δ_i^{max} - epicentral distance in km to the peak on the spectral amplitude-distance curve

Δ_i^{min} - epicentral distance in km to the trough on the spectral amplitude-distance curve

σ_0 - mean square error

σ^2 - coupling coefficient for the seismometer-galvanometer system

ACKNOWLEDGMENTS

The author wishes to express his gratitude to Dr. Stephen J. Lukasik for his review of this report and valuable comments and suggestions.

CONTENTS

I. OBSERVATION SYSTEMS AND INSTRUMENTS

The earliest seismic data on Lg were acquired and analyzed during 1961-1962 by seismographic stations located along a 3500-km-long profile extending between the Pamir Mountains and the Lena River, crossing such seismically active regions as Soviet Central Asia, Kazakhstan, Altay-Sayan and Cisbaykal [1,25]. The average distance between the 54 stations varied between 70 and 120 km. Additional data from the network of permanent stations in Central Asia and Cisbaykal were used in the determination of epicenters in those two areas. The seismic phases from 37 shallow earthquakes used in the analysis were recorded with three-component, short-period seismograph systems, mostly SKM-3, with indicator magnification between 25,000 and 120,000 (usually 50,000). The instrumental constants of the seismograph system were as follows: T_s = 1.5 or 2 s, D_s = 0.4 Cr., T_g = 0.125 - 0.2 s, D_g = 3 - 3.5 Cr., σ^2 = 0.35. The frequency-dependent part of the magnification curves of the SKM-3 seismographs used to acquire the seismic data is shown in Fig. 2.

Amplitude-distance curves of several phases including Lg from 40 crustal earthquakes of energy class K = 9.7 to 14, originating in North Tien Shan and its margins, were plotted in [2]. The earthquakes were recorded with three-component, short-period SKM-3 seismograph systems operating at 12 seismographic stations in North Tien Shan. The data from some of these stations were also used to determine attenuation of Lg [6]. The frequency-dependent part of the magnification curves of these seismographs are similar to those shown in Fig. 2. Table 1 from [3] gives the indicator magnification of these instruments at 10 of these stations.

The largest amount of very useful data on Lg analyzed in [5,6,23, 24] was acquired with the 7-channel, multiple bandpass, vertical-component ChISS seismograph operating at the Talgar station. The transducer of the ChISS seismometer at Talgar is an SVKM-3 vertical seismometer with T_s = 4 s and D_s = 0.55 driving a variable-gain, broadband, ac amplifier at unspecified gains. The amplifier output is fed simultaneously

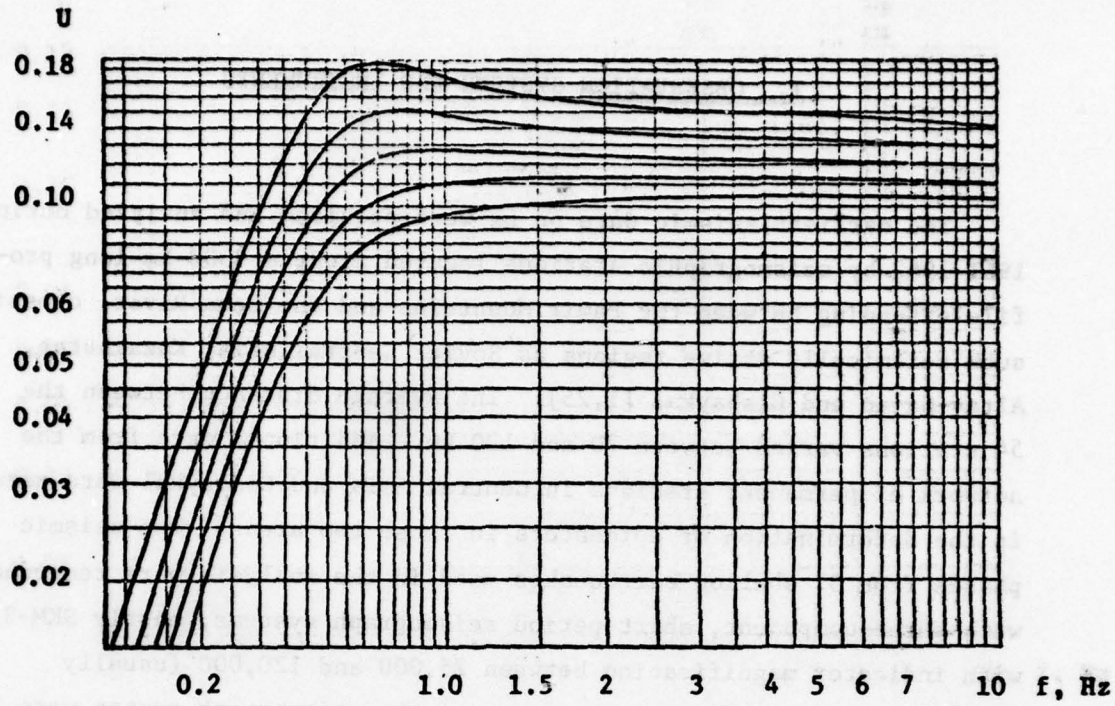

Fig. 2--The frequency-dependent part of the magnification curve (U)* of the SKM-3 seismographs used to acquire seismic data along the Pamir-Lena River profile [1]. The instrumental constants of the SKM-3 seismograph are as follows:

T_s = 2 s
D_s = 0.5 Cr.
T_g = 0.125 - 0.250 s
D_g = 4 Cr.
σ^2 = 0.35

to 7 LC filters each having a one-half octave passband and a skirt-slope of 24 dB/octave. The filter settings (high-pass and low-pass critical frequencies) and center frequencies of the ChISS seismograph at the Talgar station are given in Table 2 and the velocity sensitivity curves of this instrument are shown in Fig. 3 [4].

*The magnification (or displacement sensitivity) curve can be obtained by multiplying the frequency-dependent part of the magnification curve of the instrument by its indicator magnification. For more details see C. Shishkevish, R-1204-ARPA, *Soviet Seismographic Stations and Seismic Instruments, Part I*, May 1974, pp. 35-36.

Table 1 [3]

INDICATOR MAGNIFICATION V_o OF SKM-3 INSTRUMENTS OPERATING AT 10 SEISMOGRAPHIC EXPEDITION STATIONS IN NORTH TIEN SHAN

Station	V_o	Station	V_o
Talgar	65,900	Chilik	38,000
Kzyl-Agach	43,500	Kurmenty	34,000
Ili	40,000	Rybach'ye	25,000
Fabrichnaya	19,000	Naryn	21,000
Orto-Merke	38,000	Boamskoye ushchel'ye	52,700

Table 2 [4,5]

FILTER SETTINGS AND CENTER FREQUENCIES OF THE ChISS SEISMOGRAPH OPERATING AT THE TALGAR STATION

Channel*	Filter Settings (Hz)	Center Frequency (Hz)	
		[4]	[5,6]
1	0.24 to 0.40	0.40	0.35
2	0.55 to 0.84	0.80	0.70
3	1.1 to 1.7	1.5	1.4
4	2.2 to 3.3	2.7	2.8
5	4.6 to 7.0	5.7	5.6
6	9.2 to 14	11	11
7	18 to 29	22	22

*Certain (later?) models of ChISS seismographs were equipped with an eighth channel with filter settings of 0.2 to 0.1 Hz.

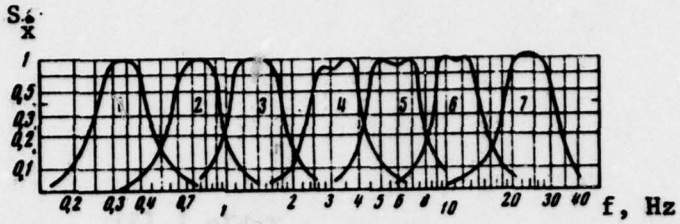

Fig. 3--Velocity sensitivity curves of the short-period, vertical-component ChISS seismograph deployed at the Talgar station in the early 1960s [4]

The several regional sets of travel times and travel-time curves of Lg obtained in [1,12,13,14] were acquired by either short-period, moderate-gain SKM-3 seismographs described above or standard Soviet broadband, intermediate-period SK seismographs with a flat displacement sensitivity curve between 1 and 10 s, usually operating at a gain of ~ 1000. The velocity amplitude spectra of Lg given in [5,6] were determined from the ChISS seismograms acquired at the Talgar station. In general, in investigating the efficiency of propagation of Lg, Soviet seismologists used seismic records obtained using ChISS seismographs operating at the Talgar, Novosibirsk, Bodon, Garm (and possibly Vremennaya) stations and either the broadband SK or short-period SKM-3 seismographs described above. The individual seismographic stations, the data from which were used in determining the efficiency of propagation of Lg in various areas of the Soviet Union, are shown in Fig. 1a,b.

II. AMPLITUDE-DISTANCE CURVES

A. GENERAL

In plotting amplitude-distance curves, it is necessary to reduce amplitudes on seismograms of earthquakes of energy class* K to a standard energy class K_o or earthquakes of surface magnitude M to a standard magnitude M_o. This requires knowledge of the variation of amplitudes with K or M, respectively. Nurmagambetov [5,7] established that the necessary relationships can be expressed in the following form:

$$\log A\,(f/K_o) = \log A\,(f/K) - \beta_K\,(f)\,(K_o - K), \quad (1)$$

$$\log A\,(f/M_o) = \log A\,(f/M) - \beta_M\,(f)\,(M_o - M), \quad (2)$$

where β_K (f) and β_M (f) are functions that decrease monotonically with frequency. The values of β_K (f) and β_M (f) for the mean frequencies of the multiple bandpass ChISS seismograph system at Talgar determined in [6] are given in Table 3. It was assumed that $\beta(f)$ is identical for all phases and all regions. It was also established that $\beta_K = 0.64\ \beta_M$.

Table 3 [5]

VALUES OF β_K AND β_M FOR THE MEAN FREQUENCIES OF THE ChISS SEISMOGRAPH SYSTEM AT TALGAR

Parameter	1	2	3	4	5	6
f, Hz	0.35	0.70	1.40	2.80	5.60	11.00
β_K	0.64	0.62	0.59	0.54	0.50	0.46
β_M	1.00	0.96	0.91	0.84	0.78	0.72

*Usually, in the case of earthquakes originating at $\Delta < 1000$ km, Soviet seismologists determine the energy class, while in the case of earthquakes recorded at $\Delta > 1000$ km, they determine the magnitude.

B. AMPLITUDE-DISTANCE CURVES OF Lg RECORDED BY SEISMOGRAPHIC STATIONS ALONG THE PAMIR-LENA RIVER PROFILE

The data used in determining the amplitude-distance curves of Lg were acquired by short-period SKM-3 seismographs installed at 54 stations along the Pamir-Lena River profile (A-A' in Fig. 1a). The amplitudes of various phases were reduced to a standard magnification of 10,000. In constructing the amplitude-distance curves, the amplitudes were normalized with respect to the amplitude of the most stable Lg phase at Δ = 1000 km in order to compensate for the different magnitudes of earthquakes.

The amplitude-distance curves of Lg and three other body waves from several earthquakes originating in Soviet Central Asia, Altay Sayan and Cisbaykal, and recorded along the Pamir-Lena River profile, are shown in Figs. 4, 5, and 6 respectively, and the composite amplitude curves for Lg for these regions and Dzhungaria are shown in Fig. 7. In Fig. 5, the amplitude curves for Lg are divided into two groups (SW, NE) according to the direction of seismic wave propagation from the earthquake epicenter to the station.

Analysis of the amplitude curves of Lg from five Soviet Central Asia earthquakes shows that the amplitudes of Lg are 4 to 5 times larger than amplitudes of Pg, but similarly to Pg decrease with distance proportionally to r^{-2} (somewhat less than $\sim r^{-2}$ at $\Delta < 400$ km). The amplitude ratios of Lg with Pg from the Altay Sayan earthquakes indicate that the amplitudes of Lg in the SW direction are close to those of Pg, while in the NE direction the amplitudes of Lg exceed those of Pg by more than an order of magnitude.

The composite amplitude-distance curves plotted in Fig. 7 show that for regions considered, the amplitude curves of Lg are similar to each other. At distances up to 700 km, the amplitudes of Lg decrease proportionately to $r^{-1.4}$. The decrease of amplitudes of Lg becomes larger at longer distances and at $r \approx 2000$ km the amplitudes of Lg decrease proportionally to $r^{-2.2}$ to $r^{-2.5}$.

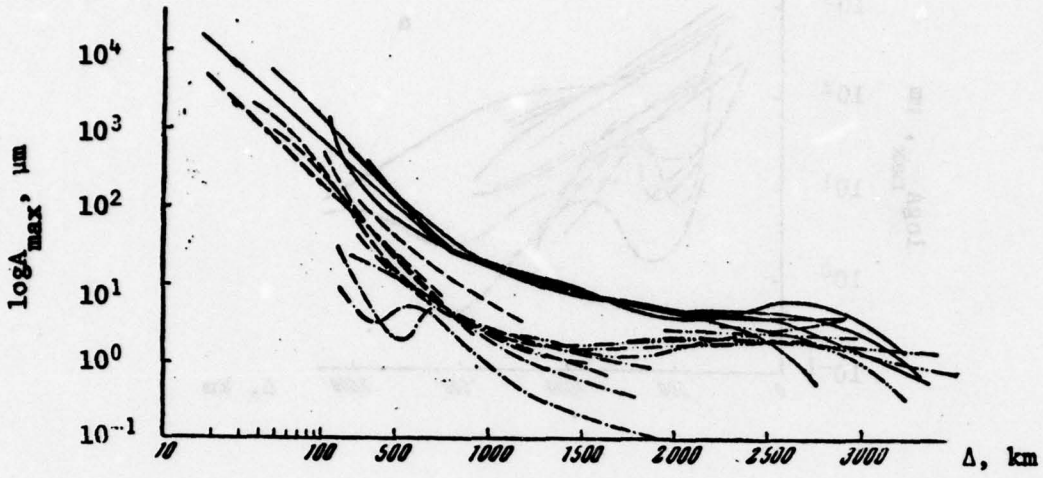

Fig. 4--Amplitude-distance curves of body waves from five earthquakes originating in Soviet Central Asia and recorded by seismographic stations located along the Pamir-Lena River profile [1]. (The distance Δ along the horizontal at Δ ≤ 100 km is plotted on a logarithmic scale.)

_____ Lg

------ Pg

-·-·-· Pn

-··-·· P

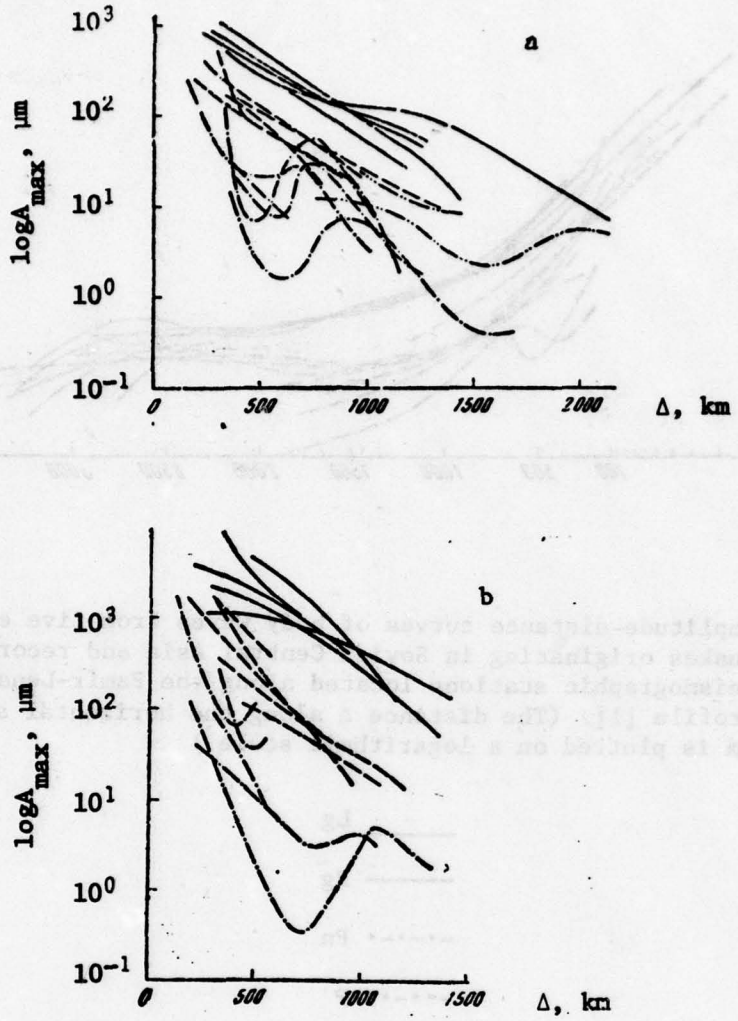

Fig. 5 --Amplitude-distance curves of body waves originating in Altay-Sayan recorded by seismographic stations located along the Pamir-Lena River profile [1]

a--seismic waves propagating in the SW direction; b--seismic waves propagating in the NE direction

——— Lg -.-.-.- Pn
- - - Pg -..-..-..- P

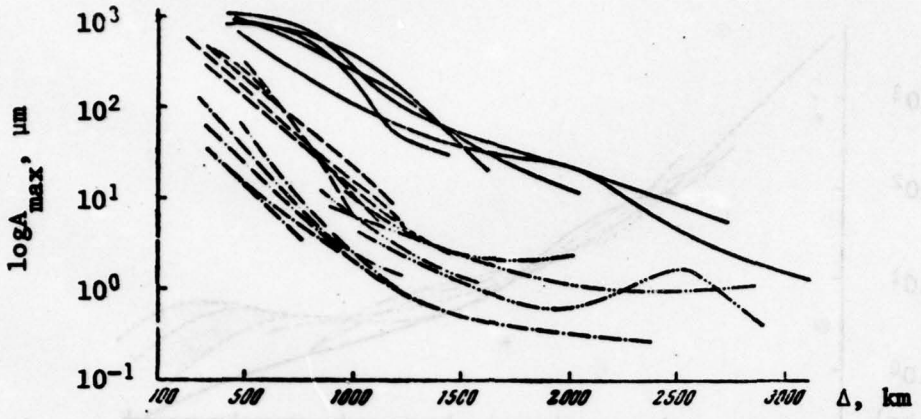

Fig. 6--Amplitude-distance curves of body waves from five earthquakes originating in Cisbaykal and recorded by seismographic stations located along the Pamir-Lena River profile [1]

——— Lg

- - - Pg

-·-·-· Pn

-··-·· P

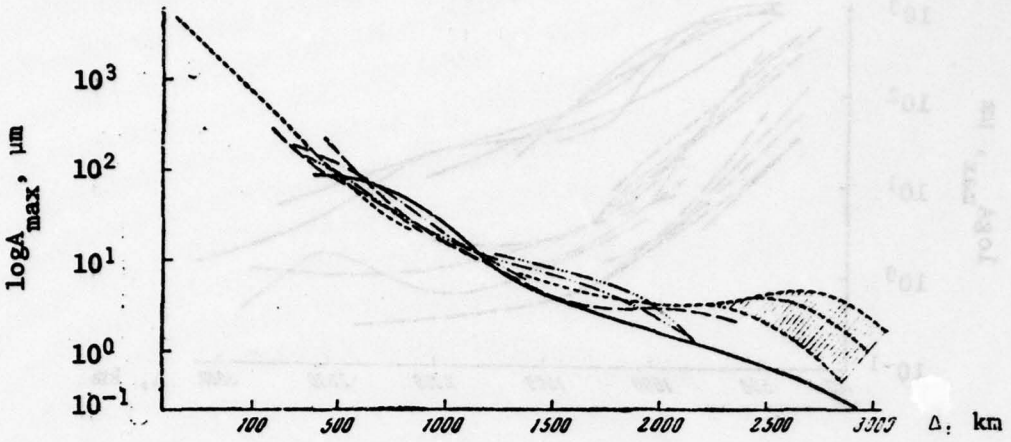

Fig. 7--Composite amplitude-distance curves of Lg from earthquakes originating in Central Asia (1); Dzhungaria (2); Altay Sayan, NE of the epicenters (3) and SW of the epicenters (4); Eastern Sayan (5) and Cisbaykal (6) and recorded along the Pamir-Lena River profile [1]. (The distance Δ along the horizontal at Δ ≤ 100 km is plotted on a logarithmic scale.)

-------- 1

-·-·-·- 2

-·-·-·-·- 3

-··-··-·· 4

_ _ _ _ _ 5

_____ 6

C. AMPLITUDE-DISTANCE CURVES OF Lg RECORDED BY NORTH TIEN SHAN SEISMOGRAPHIC STATIONS

The amplitude distance curves of Lg and three other phases from 40 crustal earthquakes originating in North Tien Shan and recorded by seismographic stations equipped with SKM-3 instruments in that region (see Fig. 1b) are plotted in Fig. 8 [2]. Three amplitude curves were constructed for each of the three predominant directions of propagation from a group of earthquake epicenters to the station. Figure 8 also shows the composite amplitude curve for all directions which, for convenience, is also plotted on a separate figure (Fig. 9). In constructing amplitude-distance curves, the peak amplitudes were reduced to the energy class K = 11 and normalized to a standard distance.

From Fig. 8 it can be seen that the shape of the amplitude-distance curve of Lg in the NE direction is similar to that in the SW direction. However, the amplitude curve in the N direction differs considerably from the other two; it displays a peak at distances at which the two other amplitude curves have a weak minimum.

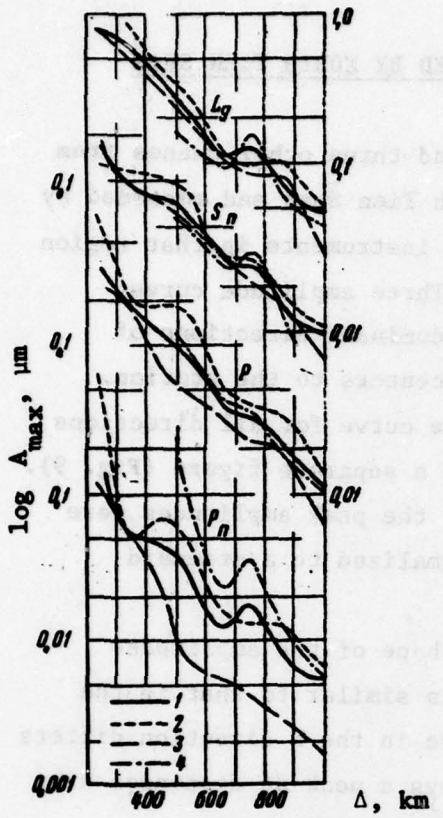

Fig. 8--Amplitude-distance curves of Lg and three other phases from earthquakes originating in Tien Shan and recorded in the same area [2]

1-composite curve;
2-seismic waves propagating in the SE direction relative to the station
3-seismic waves propagating in the SW direction relative to the station
4-seismic waves propagating in the N direction relative to the station

Fig. 9--Composite amplitude-distance curves for Lg and three other phases from earthquakes originating in North Tien Shan and recorded by seismographic stations in that region [2]

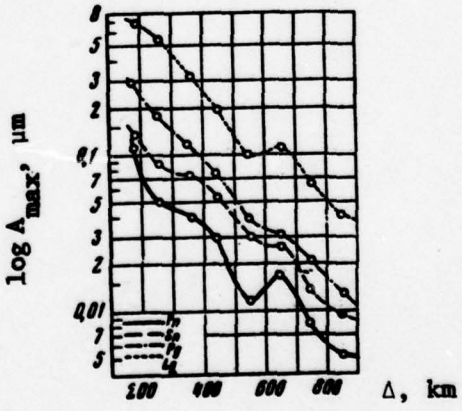

D. SPECTRAL AMPLITUDE DISTANCE CURVES OF Lg RECORDED BY THE ChISS SYSTEM AT THE TALGAR STATION

The first of the two papers containing spectral amplitude-distance curves of Lg recorded by a multiple-bandpass ChISS velocity seismograph was published by Nurmagambetov [5]. The amplitude curves were obtained for each of the seven channels of the ChISS system operating at the Talgar station (7 in Fig. 1a) by averaging Lg amplitudes reduced to energy class $K_0 = 10$, using formula (1). Since only the seismograms acquired at a single station were used, the spectral amplitude-distance curves shown in Fig. 10 reveal only the general variation (slope) of the curves rather than the fine details. The averaging was performed on a computer with the standard deviation of individual points from the mean curve not exceeding 0.3 to 0.4 logarithmic unit. For convenience, the curves for the different frequencies are displaced relative to each other. The absolute amplitudes are denoted by horizontal lines that correspond to the absolute values of $A/T = 0.1$ μm/s.

From Fig. 10 it can be seen that the curves can be divided into three sectors, corresponding to epicentral distance ranges Δ = 20-100 km, 100-300 km and 300-800 km. The first sector is characterized by a regular increase of the slope of the curve (-N) with frequency. At Δ > 100-120 km the slopes of the high-frequency curves diminish and the low-frequency curves become more nearly horizontal. As the frequency increases, the location of this relatively flat sector is displaced toward shorter distances. The values of the slope (-N) of the six spectral amplitude-distance curves plotted in Fig. 10 are given in Table 4 for various epicentral-distance ranges. The differences between the amplitude curves for different azimuths with respect to the Talgar station are small and appeared only at high frequencies. In general, attenuation is somewhat higher for Lg propagating across geological structures.

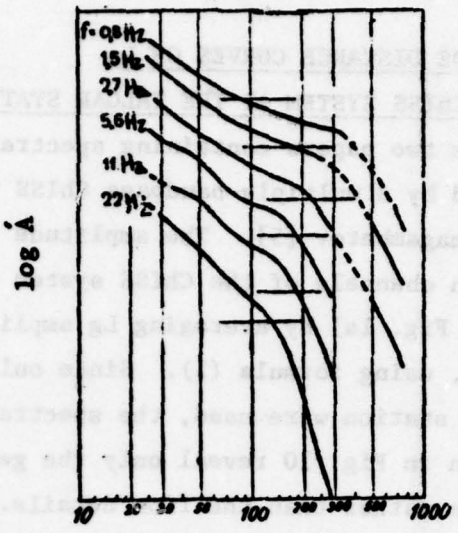

Fig. 10--Spectral amplitude-distance curves for Lg phases recorded by the multiple bandpass ChISS system at the Talgar station [5]. The numbers on the left indicate the mean frequency of the channel in Hz. The intersection of the line with each curve is at the point where the amplitude of the Lg is 0.1 μm/s.

Table 4 [5]

THE VALUES OF SLOPE (-N) OF THE SIX SPECTRAL AMPLITUDE CURVES SHOWN IN FIG. 10 FOR VARIOUS EPICENTRAL DISTANCE RANGES

Δ , km	Frequency, Hz					
	0.8	1.5	2.7	5.7	11	22
20-100	1.2	1.3	1.4	1.5	1.6	2.0
100-160	-	-	0.8	0.9	-	-
160-300	-	-	2.5	3.6	5.3	8.4
120-300	0.7	0.8	-	-	-	-
300-800	3.7	3.7	3.8	-	-	-

The second and much more detailed analysis of the spectral amplitude-distance curves of Lg recorded by the ChISS system at Talgar (7 in Fig. 1a) was included in the monograph by Antonova, et al. [6]. Depending on direction from the Talgar station to the epicenter, the earthquakes were divided into the following four groups: northeast (NE), east (E), south (S) and west (W).

The spectral amplitude-distance curves of Lg phases for each of the four directions were constructed from the records of numerous earthquakes with epicentral distances covering the range of interest, using Nersesov and Rautian's travel time data given in Table 9 (see also Fig. 14). The spectral amplitude-distance curves at six mean frequencies were obtained by measuring amplitude peaks of Lg over 15 to 20 s intervals of traces recorded by six channels* of the seven channel bandpass ChISS seismograph system. At $\Delta \leq 1000$ km the peaks are reduced to the reference energy class $K_o = 10$, while at longer epicentral distances the spectral amplitudes are reduced to the reference magnitude $M_o = 5$, using formulas (1) and (2), respectively.

The spectral amplitude-distance curves of Lg are shown in Fig. 11, and their most important parameters are listed in Table 5. In Table 5 -N is the slope of the curve within the specified distance range and Δ_i^{max} and Δ_i^{min} are the epicentral distances in km to the peaks and troughs on the curves, respectively. The values of these parameters were determined for the following three frequency ranges: 0.35 to 0.7, 1.4 to 2.8 and 5.6 to 11 Hz, which in abbreviated notation will be denoted by their center frequencies: 0.5, 2 and 8 Hz.

The spectral amplitude-distance curves of Lg shown in Fig. 11 display oscillatory behavior which, however, is not as pronounced as it is for compressional waves. These curves for the western direction are monotonic and at distances $\Delta \leq 1000$ km do not display oscillatory behavior. The spectral amplitude-distance curves can be divided into several characteristic sectors.

---

*High attenuation made it impossible to obtain records from the high frequency (seventh) channel ($\bar{f} = 22$ Hz).

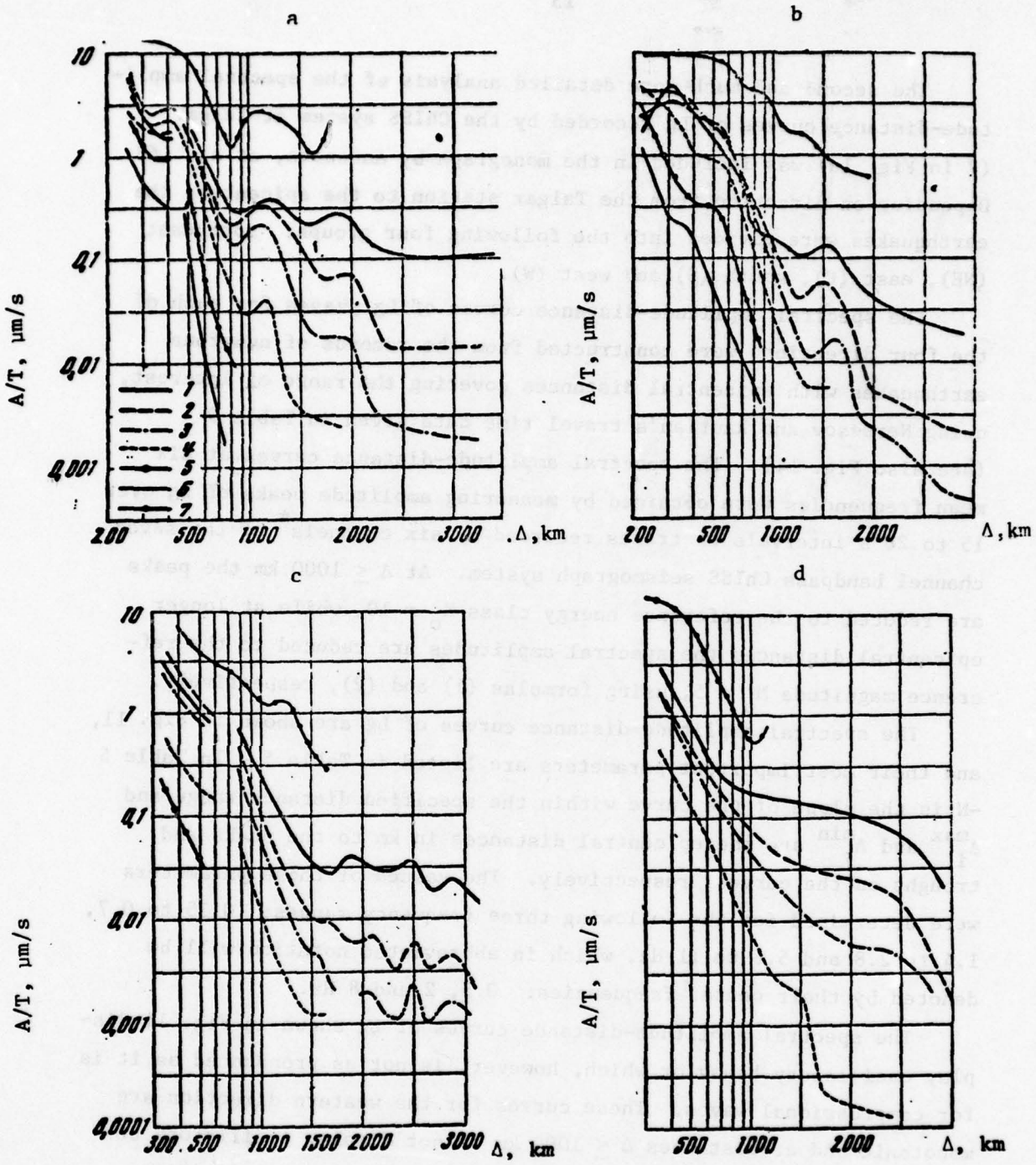

Fig. 11--Spectral amplitude-distance curves for Lg phases for the northeastern (a), eastern (b), southern (c) and western (d) directions

1--$\bar{f}$ = 0.35 Hz, 2--$\bar{f}$ = 0.7 Hz, 3--$\bar{f}$ = 1.4 Hz, 4--$\bar{f}$ = 2.8 Hz, 5--$\bar{f}$ = 5.6 Hz, 6--$\bar{f}$ = 11 Hz, 7--from records of wideband SK seismographs

Table 5 [6]

PARAMETERS OF SPECTRAL AMPLITUDE-DISTANCE CURVES OF Lg PHASES FOR FOUR DIRECTIONS OF PROPAGATION AND THREE CENTER FREQUENCIES

Parameter	Distance, km	NE			E		
		0.5 Hz	2 Hz	8 Hz	0.5 Hz	2 Hz	8 Hz
$-N_1$	300-600	2.5	5	4	-	2	4.5
$-N_2$	500-1000	4.5	6.5	11	5.0	6.5	6.5
A/T	800	250	100	3	300	200	14
A/T	1500	200	10	-	100	10	-
Δ_3^{min}	-	850	900	-	1250	1350	-
Δ_3^{max}	-	1100	1150	-	1500	1600	-
Δ_3^{max}	-	1900	1900	-	-	-	-
Parameter	Distance, km	S			W		
		0.5 Hz	2 Hz	8 Hz	0.5 Hz	2 Hz	8 Hz
$-N_1$	300-600	2.7	3.0	4.0	3.6	3.8	-
$-N_2$	500-1000	5.5	6.5	-	(2.5)	(3.3)	-
A/T	800	500	100	-	120	20	-
A/T	1500	20	2	-	80	5	-
Δ_3^{min}	-	1600	1500	-	-	-	-
Δ_3^{max}	-	2000	2000	-	-	-	-
Δ_3^{max}	-	2500	2500	-	-	-	-

The initial sector to $\Delta \simeq 350$, 400 and 550 km for the NE, E and S directions, respectively, is characterized by relatively weak attenuation and weak frequency dependence of N_1. The NE curves display a peak in the distance range $\Delta_1 \simeq 350$ to 450 km. The spectral amplitude-distance curves along the sector Δ_2 decrease monotonically and $-N_2 \simeq 5$ to 7. The sectors Δ_2 of the curves cover the distance ranges of 500 to 800, 600 to 1200, 800 to 1500 and 700 to 1500 km in the NE, E, S, and W directions, respectively. The slope of the curve ($-N_2$) gradually decreases from NE to W.

In the distance range between 800 and 1500 to 2000 km attenuation is highly frequency dependent. For example, while the amplitudes of the spectral amplitude-distance curves in the NE and E directions at frequencies of 0.35 and 2.8 Hz are approximately equal at a distance of 500 km, at 1500 km they differ by 1.5 to 2 orders of magnitude. The end part of the sector Δ_2 displays oscillatory behavior, most clearly observed in the NE direction. As the distance toward the epicentral region increases, the positions of troughs, Δ_3^{min}, and peaks, Δ_3^{max}, on the spectral amplitude-distance curve are gradually shifted toward longer distances. At the same time, the amplitude of the oscillation decreases. A small peak, Δ_4^{max}, on the curves for the southern and western directions occurs at distances of 2000 to 2500 km.

The amplitudes of Lg at $\Delta \leq 1000$ km are approximately the same for all but the western direction where the amplitude level is 1.5 to 2 times lower. In the distance range 1500 to 2000 km, Lg propagates most efficiently in the northeastern direction and least efficiently in the southern direction.

The standard deviation of the A/T data was determined to be frequency independent for all phases. It was estab ished that at distances up to 1000 km, Lg phase is scattered less than the other phases. Scattering increases considerably in the northeastern direction at distances exceeding 1000 km but remains low in the southern direction.

Analysis of scattering of A/T data indicates that the accuracy of determining the magnitudes of earthquakes can be improved by using an amplitude-distance correction curve constructed from Lg or Pg for earthquakes originating at distances up to 1000 km and a curve

constructed from P for earthquakes occurring at distances exceeding 1000 km. A significant increase in accuracy may also be attained by utilizing several bandpass channels.

III. ATTENUATION

A. GENERAL

For a uniform point source of elastic waves in a spherical earth, the amplitudes of the Airy phase in the time domain are given by

$$A = k\Delta^{-1/3} (\sin\Delta)^{-1/2} \exp(-\gamma\Delta), \qquad (3)$$

where A is the amplitude at epicentral distance Δ; k is a constant; γ is the coefficient of inelastic attenuation, $\gamma = \Pi/VgTQ$; Vg is the group velocity and Q is the specific quality factor. The inelastic attenuation coefficient of the Airy phase can be determined by matching theoretical attenuation (amplitude-distance) curves, determined from formula (3) for various values of γ and plotted on a log-log scale, with the mean experimental amplitude-distance curve. Over a limited range of distances the attenuation curve can be approximated by a straight line with a slope -N. Thus, within this range, the amplitude of the seismic wave

$$A \sim \Delta^{-N} \qquad (4).$$

B. Q-FACTORS

The data recorded by broadband SK instruments at a group of stations in North Tien Shan (see Fig. 1b) were used to determine the attenuation of Lg in Soviet Central Asia [6]. Assuming that Lg represents a higher mode wave traveling with minimum group velocity, formula (3) was used in an attempt to obtain the theoretical attenuation curve to fit the data. However, it was established that the experimental data are best approximated by two curves: $\gamma = 0.20$ deg^{-1} curve for $\Delta < 1000$ km and $\gamma = 0.13$ deg^{-1} curve for $\Delta > 1000$ km. Using $T \simeq 3$ s, $Vg = 3.57$ km/s for $\Delta < 1000$ km and $Vg = 3.65$ km/s for $\Delta > 1000$ km, one obtains the following Q-values for the 3 s period Lg phase:

$Q \simeq 160$, $\Delta < 1000$ km; $Q \simeq 250$, $\Delta > 1000$ km.

A crude straight line approximation to the two curves shows that Lg is attenuated proportionally to $\Delta^{-1.6}$, which is very close to that for Rayleigh waves ($\Delta^{-1.66}$) at long epicentral distances [6].

The oscillatory structure of the amplitude-distance curves constructed from seismograms of multiple-bandpass ChISS systems makes it difficult to estimate attenuation of Lg. A very rough estimate of the quality factors of Lg for three different period values from the change in the shape of ChISS spectra of Lg with the epicentral distance was made in [8]. It was based on data acquired at the Talgar, Bodon and Novosibirsk seismographic stations (see Fig. 1a) from earthquakes originating roughly NE, E and S (but north of the Tibetan plateau) of these stations. It was estimated that

$Q \simeq 300$ to 400, $T = 1.0$ to 2.5 s;

$Q \simeq 600$ to 800, $T = 0.4$ to 1.0 s;

$Q \simeq 1000$ to 1300, $T = 0.2$ to 0.5 s.

The Q-factors for Lg thus exhibit strong frequency dependence, increasing greatly with increasing frequency.

Amplitude-distance curves of unspecified TNT explosions* fired in Soviet Central Asia were used by Pasechnik [9] to estimate the Q-factor of Lg, in the range $\Delta = 150$ to 1500 km. Using $T = 0.8$ s and $V_g = 3.55$ km/s, he determined that

$Q \simeq 190$, $\Delta = 150$ to 1500 km.

---

*See footnote on pp. 22-23 of this report for comments on these explosions.

IV. MAGNITUDE RELATION

The magnitude relation most frequently used by Soviet seismologists is the Gutenberg-Richter formula

$$M = \log_{10} (A/T) + Q_M (\Delta) \quad (5)$$

where A/T is the ratio of the amplitude to period and $Q_M (\Delta)$ is the amplitude-distance correction factor, i.e., an empirical attenuation curve. The amplitude-distance correction factors for Lg of shallow earthquakes recorded by broadband SK instruments at a group of stations in North Tien Shan (Fig. 1b) are given in Table 6 [6]. Their values were determined from the maximum A/T values of Lg, $(A/T)_{max}$, where A is the zero-to-peak amplitude of Lg on seismograms of either a horizontal- or vertical-component SK seismograph, displaying maximum amplitude.

In a monograph on seismic effects of nuclear explosions [9], Pasechnik refers to an unspecified amplitude-distance correction factor*, $Q_M (\Delta)$, determined from maximum Lg_1 motion generated by underground (nuclear) explosions recorded by horizontal seismographs. Using unspecified seismic data, he estimates that the ratio of the trace amplitude of Lg on the horizontal component seismogram with that on the vertical component is 1.5 ± 0.15. Thus, the $Q_M (\Delta)$ curve can be used with seismograms obtained with vertical seismographs to determine M_{Lg}, the vertical-component magnitude of Lg, with an error not exceeding 0.15 magnitude units.

Using this technique, Pasechnik calculates M_{Lg} of six shallow earthquakes originating in Soviet Central Asia plotted in Fig. 12 and two TNT explosions† in the same region and compares them with body-wave magnitudes of the same events determined from Pn, (m_{Pn}) and

---

*Probably determined from the following formula for Lg from underground nuclear explosions in Nevada:

$$M = \log (A/T) + 3 \log r - B,$$

where B = 2.65. This formula was published in a paper by R. G. Baker, "Preliminary Study for Determining Magnitude from Lg," *Earthquake Notes*, Seismology Society of America, Vol. 38, No. 1, pp. 23-28.

†Throughout the book [9], Pasechnik refers to two large chemical explosions detonated in Soviet Central Asia. According to the original

Table 6 [6]

AMPLITUDE-DISTANCE CORRECTION FACTORS
FOR Lg FROM SHALLOW EARTHQUAKES

Δ (km)	Q_M	Δ (km)	Q_M	Δ (km)	Q_M
200	4.34	1000	5.55	1800	5.90
300	4.57	1100	5.55	1900	5.94
400	4.78	1200	5.56	2000	6.00
500	4.98	1300	5.60	2100	6.05
600	5.15	1400	5.67	2200	6.12
700	5.30	1500	5.73	2300	6.20
800	5.42	1600	5.80	2400	6.28
900	5.50	1700	5.86	2500	6.38
				2600	6.50

$P^*(m_{p^*})$. These magnitudes and differences between them are plotted in Table 7. It can be seen from this table that the magnitudes M_{Lg_1} of the two TNT explosions determined using this technique are in complete agreement with m_{Pn} and m_{P^*} for the same two events. However,

---

Russian version of Table 7 (Table 44 on p. 169 in the Russian text), these two explosions are plotted on Fig. 12 (Fig. 32 on p. 76 in the Russian text). However, Fig. 32 shows only locations of the six local earthquakes, black dots numbered 1 through 6, and eleven seismographic stations ●. The symbols keyed to the legend also include a circle that the legend identifies as an unspecified and unreferred to earthquake. It is very likely that the circle actually denotes one of the two chemical explosion sites. No additional data could be found in the Soviet scientific literature on this explosion. A very likely candidate for the second event is the Arys cratering explosion detonated on 19 December 1957 at 09 hr 00 min 00s G.T. in the Kabulsay region of the Arys sector of the Tashkent railroad (φ = 42°12'15"N, λ = 69°03'02"E). One kt of conventional explosives was placed into a chamber at a depth of 40 m. According to Soviet estimates, the magnitude of this event was $M_s = 3.9 \pm 0.1$, $m_b = 5.0$. The magnitude of this event recorded by an Uppsala station is $m_b = 5.1$. This is close to $m_b = 4.8$ given in [9] for one of its chemical explosions. The Arys event was recorded by most of the stations shown in Fig. 12 and its site would be located in the upper left corner of Fig. 12.

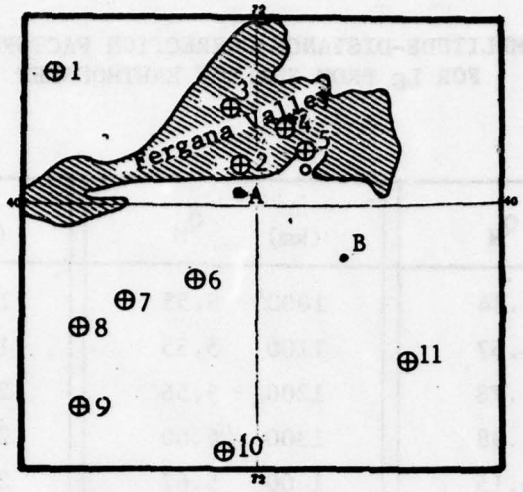

Fig. 12--Epicenters of earthquakes used in determining travel time curves shown in Figs. 18 and 19 [9]

o--possible location of one explosion, ●--earthquake, ⊕--seismographic station (numerical listing follows)

1--Tashkent (41°20'N,69°18'E); 2--Fergana (40°23'N,71°47'E); 3--Namangan (40°59'N,71°40'E); 4--Andizhan (40°45'N,72°22'E); 5--temporary station; 6--Dzhergatal' (39°13'N,71°14'E); 7--Garm (39°00'N,70°19'E); 8--Obi-Garm (38°43'N,69°43'E); 9--Kulyab (37°54'N,69°45'E); 10--Khorog (37°29'N,71°32'E); 11--Murgab (38°22'N,73°56'E)

while m_{Lg_1} of the six earthquakes are generally in good agreement with m_{Pn} for the same events, both m_{Lg_1} and m_{Pn} differ significantly from m_{P*}. (~0.5 magnitude unit). Lack of data, very confusing text and the use of a very "dubious" technique (formula for M_{Lg_1} probably applies only to Nevada events recorded at short epicentral distances and the ratio of trace amplitudes of horizontal motion of Lg with vertical motion is assumed to be a constant equal to 1.4 ± 0.5) throw a great deal of doubt on the significance of Pasechnik's calculations.

Table 7 [9]

m_{Pn}, m_{P*} AND m_{Lg} MAGNITUDES AND DIFFERENCES BETWEEN THESE MAGNITUDES FOR SIX EARTHQUAKES AND TWO TNT EXPLOSIONS IN THE SAME REGION OF SOVIET CENTRAL ASIA

Source	No. on Fig. 11	m_{Pn}	m_{P*}	m_{Lg}	$m_{Pn} - m_{P*}$	$m_{Lg} - m_{P*}$	$m_{Lg} - m_{Pn}$
TNT Explosion	-	4.4	4.4	4.4	0	0	0
	-	4.8	4.8	4.8	0	0	0
Earthquake	1	-	4.0	4.7	-	0.7	-
	2	4.7	4.2	4.8	0.5	0.6	0.1
	3	5.6	5.1	5.6	0.5	0.5	0
	4	4.5	4.0	4.5	0.5	0.5	0
	5	4.5	4.0	4.6	0.5	0.6	0.1
	6	4.5	3.8	4.2	0.7	0.4	-0.3

V. TRAVEL TIMES

In a 1963 paper [10], Pataraya used seismograms of 200 earthquakes recorded at the Tbilisi, Simferopol', Sochi and other seismographic stations to construct travel time curves of Lg and Rg at Δ = 200 to 1500 km. Unfortunately, this paper is unavailable. According to [11], Pataraya determined that the velocity and period of Lg_1 and Lg_2 are as follows:

$$V_{Lg_1} = 3.49 \text{ km/s}, T = 1.5 \text{ to } 8 \text{ s}; V_{Lg_2} = 3.28 \text{ km/s}; T = 6 \text{ to } 14 \text{ s}.$$

In a paper published in 1961 [12], Val'dner used 120 seismograms of earthquakes recorded mostly by broadband SK seismographs at base stations in the USSR to determine the approximate travel times of Lg_1 and Lg_2 at 5° intervals in the distance range Δ = 10 to 55°. The times of Lg_1 - P and Lg_2 - P are given in Table 8 and plotted in Fig. 13.

The most accurate travel times of Lg phases were determined by Nersesov and Rautian [1] using data acquired during 1961-1962 by 54 seismographic stations located along the 3500-km-long profile extending between the Pamir Mountains and Lena River (A-A' in Fig. 1a). The three unidentified Lg phases labeled $S\overset{1}{g}(L\overset{1}{g})$, $S\overset{2}{g}(L\overset{2}{g})$ and $S\overset{3}{g}(L\overset{3}{g})$ were determined for two directions measured from the profile to the earthquakes: northeast (Siberia) and southwest. The travel times of Lg for the two directions are given in Table 9 and the travel time curves of all phases recorded along the profile are plotted in Fig. 14.

Nersesov and Rautian's analysis of seismic data acquired along the Pamir Mountains-Lena River profile [1] showed that, in general, the direct shear wave $\overline{S}$ was clearly observed on seismograms, beginning very near the epicenter. As is frequently the case, the emergence of Lg could not be identified and the shear wave with a velocity of 3.5 km/s recorded at $\Delta < 250$ km was assumed to be the $\overline{S}$ phase while at $\Delta \geq 250$ km it was assumed to be Lg. The velocity of Lg observed

Table 8 [12]

TIMES OF Lg_1 - P AND Lg_2 - P, IN SECONDS

Δ°	$t_{Lg_1} - t_P$	$t_{Lg_2} - t_P$	Δ°	$t_{Lg_1} - t_P$	$t_{Lg_2} - t_P$
10	170	192	35	685	765
15	258	292	40	801	892
20	355	401	45	918	1021
25	463	520	50	1035	1149
30	573	641	55	1153	1279

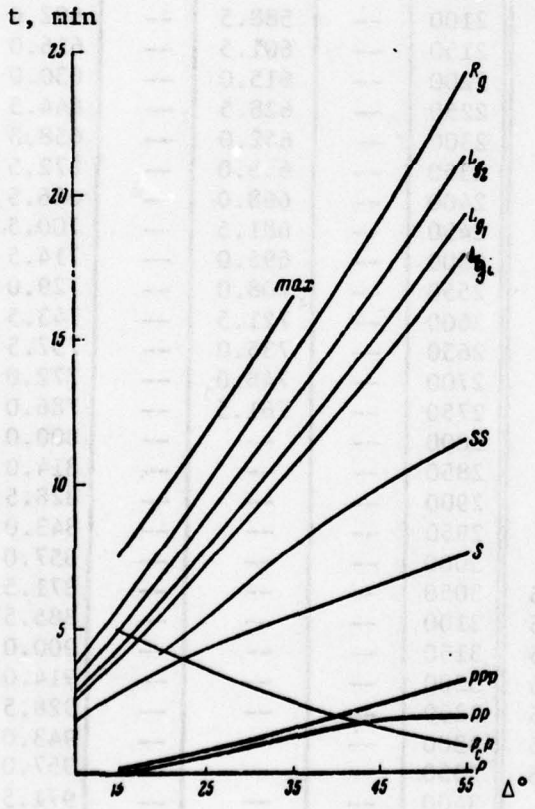

Fig. 13--Travel time curves of Lg_i - P, Lg_1 - P, Lg_2 - P, Rg - P, M - P, PcP - P, PP - P, PPP - P, S - P and SS - P [12]

Table 9 [1]

TRAVEL TIMES OF Lg
ALONG THE PAMIR-LENA RIVER PROFILE

Δ (km)	L_g^1 (s)		L_g^2 (s)	L_g^3 (s)	Δ (km)	L_g^1 (s)		L_g^2 (s)	L_g^3 (s)
	WEST	SIBERIA				WEST	SIBERIA		
300	84.5	--	87.0	--	1850	--	521.5	--	531.0
350	98.5	--	101.5	--	1900	--	535.0	--	545.0
400	112.5	--	116.0	--	1950	--	548.5	--	559.0
450	126.5	--	130.0	--	2000	--	562.0	--	573.5
500	140.5	--	174.5	--	2050	--	575.0	--	587.5
550	154.5	--	159.0	--	2100	--	588.5	--	602.0
600	168.5	--	173.5	--	2150	--	601.5	--	616.0
650	182.5	--	188.0	--	2200	--	615.0	--	630.0
700	196.5	--	202.5	--	2250	--	628.5	--	644.5
750	210.5	--	217.0	--	2300	--	642.0	--	658.5
800	224.5	--	232.0	--	2350	--	655.0	--	672.5
850	238.5	--	246.5	--	2400	--	668.0	--	686.5
900	252.5	--	261.0	--	2450	--	681.5	--	700.5
950	266.5	--	275.0	--	2500	--	695.0	--	714.5
1000	280.5	--	289.0	--	2550	--	708.0	--	729.0
1050	294.0	--	303.0	--	2600	--	721.5	--	743.5
1100	308.0	--	317.5	--	2650	--	735.0	--	757.5
1150	322.0	--	332.0	--	2700	--	748.0	--	772.0
1200	335.5	--	346.0	--	2750	--	761.5	--	786.0
1250	349.5	--	360.0	--	2800	--	--	--	800.0
1300	363.0	--	373.5	--	2850	--	--	--	814.0
1350	376.5	--	387.5	--	2900	--	--	--	828.5
1400	390.0	--	401.5	--	2950	--	--	--	843.0
1450	404.0	--	415.0	--	3000	--	--	--	857.0
1500	418.0	--	429.0	432.5	3050	--	--	--	871.5
1550	432.0	--	443.0	446.5	3100	--	--	--	885.5
1600	445.5	--	457.0	460.5	3150	--	--	--	900.0
1650	459.0	467.5	470.5	474.5	3200	--	--	--	914.0
1700	--	481.5	484.5	488.5	3250	--	--	--	928.5
1750	--	495.5	498.0	502.5	3300	--	--	--	943.0
1800	--	508.5	--	516.5	3350	--	--	--	957.0
					3400	--	--	--	971.5

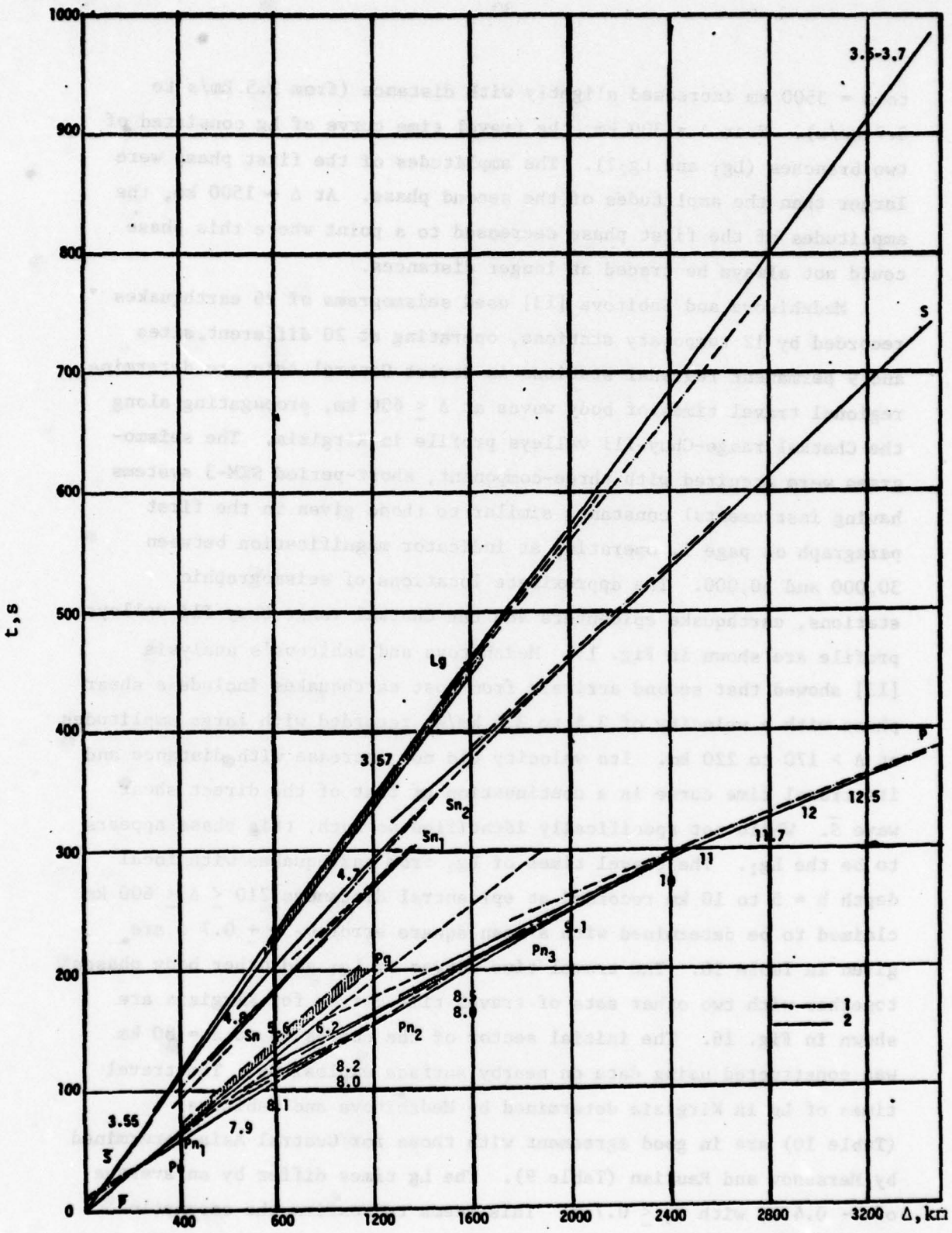

Fig. 14--Travel time curves of phases recorded along the Pamir-Lena River profile [1]

1 - West, 2 - Siberia (numbers indicate apparent velocities in km/s)

to Δ = 3500 km increased slightly with distance (from 3.5 km/s to 3.7 km/s). Near Δ = 300 km, the travel time curve of Lg consisted of two branches (Lg_1 and Lg_2?). The amplitudes of the first phase were larger than the amplitudes of the second phase. At $\Delta \sim 1500$ km, the amplitudes of the first phase decreased to a point where this phase could not always be traced at longer distances.

Medzhitova and Sabitova [13] used seismograms of 26 earthquakes recorded by 12 temporary stations, operating at 20 different sites and 9 permanent regional stations in Soviet Central Asia, to determine regional travel times of body waves at $\Delta \leq 600$ km, propagating along the Chatkal range-Chuy-Ili valleys profile in Kirgizia. The seismograms were acquired with three-component, short-period SKM-3 systems having instrumental constants similar to those given in the first paragraph on page 1, operating at indicator magnification between 30,000 and 50,000. The approximate locations of seismographic stations, earthquake epicenters and the Chatkal range-Chuy-Ili valleys profile are shown in Fig. 15. Medzhitova and Sabitova's analysis [13] showed that second arrivals from most earthquakes include a shear phase with a velocity of 3.5 to 3.6 km/s, recorded with large amplitudes at Δ > 170 to 220 km. Its velocity did not increase with distance and its travel time curve is a continuation of that of the direct shear wave $\overline{S}$. While not specifically identified as such, this phase appears to be the Lg_1. The travel times of Lg_1 from earthquakes with focal depth h = 5 to 10 km recorded at epicentral distances $210 \leq \Delta \leq 600$ km claimed to be determined with a mean square error $\sigma_0 = \pm 0.7$ s are given in Table 10. The travel time curves of Lg_1 and other body phases together with two other sets of travel time curves for Kirgizia are shown in Fig. 16. The initial sector of the curves up to Δ = 80 km was constructed using data on nearby surface explosions. The travel times of Lg in Kirgizia determined by Medzhitova and Sabitova (Table 10) are in good agreement with those for Central Asia determined by Mersesov and Rautian (Table 9). The Lg times differ by an average of $\sim$ 0.4 s, with $\sigma_0 \leq 0.7$ s. This seems to confirm the assumption that the shear wave with a velocity of 3.5 to 3.6 km/s is the Lg_1 phase.

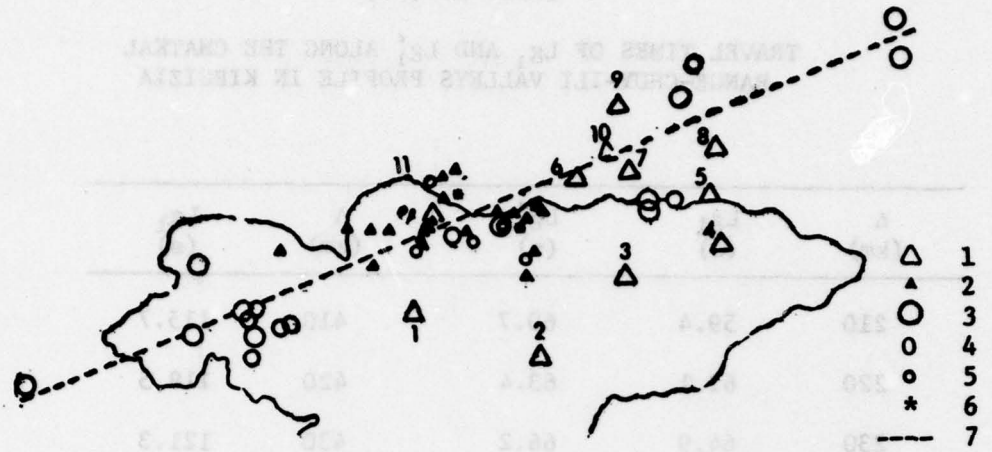

Fig. 15--Locations of seismographic stations and earthquakes used in determining the travel times of Lg_1 [13]

△ 1--permanent station
▲ 2--temporary station site
○ 3--epicenter of earthquake of K = 11 to 12
0 4--epicenter of earthquake of K = 9 to 10
o 5--epicenter of earthquake of K = 7 to 10
* 6--explosion site used in determining times at $\Delta \leq 150$ km
---- 7--Chatkal range-Chuy-Ili-valleys profile

Permanent stations: 1--Aral; 2--Naryn; 3--Kadzhi Say; 4--Przheval'sk; 5--Kurmenty; 6--Fabrichnaya; 7--Talgar; 8--Chilik; 9--Ili; 10--Alma-Ata; 11--Frunze.

Tsibul'chik [14] used seismograms from 24 earthquakes recorded by as many as 16 permanent and temporary seismographic stations in the Altay-Sayan and Tuva regions of Siberia to determine regional travel times. The data were acquired with SKM-3 seismographs operating at indicator magnification of ~ 40,000. The predominant phase recorded at Δ = 230 - 1000 km with a velocity of the $\bar{S}$ phase (3.56 km/s), the formation of which was attributed by the author to superposition of multiples, is probably the Lg phase. The travel time curves of this phase, assumed to be the Lg, and other body waves for the Altay-Sayan region, are plotted in Fig. 17.

Table 10 [13]

TRAVEL TIMES OF Lg_1 AND Lg_1' ALONG THE CHATKAL RANGE-CHUY-ILI VALLEYS PROFILE IN KIRGIZIA

Δ (km)	Lg_1 (s)	Lg_1' (s)	Δ (km)	Lg_1 (s)
210	59.4	60.7	410	115.7
220	62.1	63.4	420	118.5
230	64.9	66.2	430	121.3
240	67.7	69.0	440	124.0
250	70.6	71.9	450	126.9
260	73.5	74.8	460	129.7
270	76.2	77.5	470	132.6
280	79.1	80.4	480	135.3
290	82.0	83.3	490	138.1
300	84.9	86.2	500	140.9
310	87.9		510	143.6
320	90.7		520	146.5
330	93.3		530	149.3
340	96.1		540	152.1
350	99.0		550	154.9
360	101.7		560	157.5
370	104.5		570	160.3
380	107.3		580	163.1
390	110.1		590	165.8
400	112.8		600	168.6

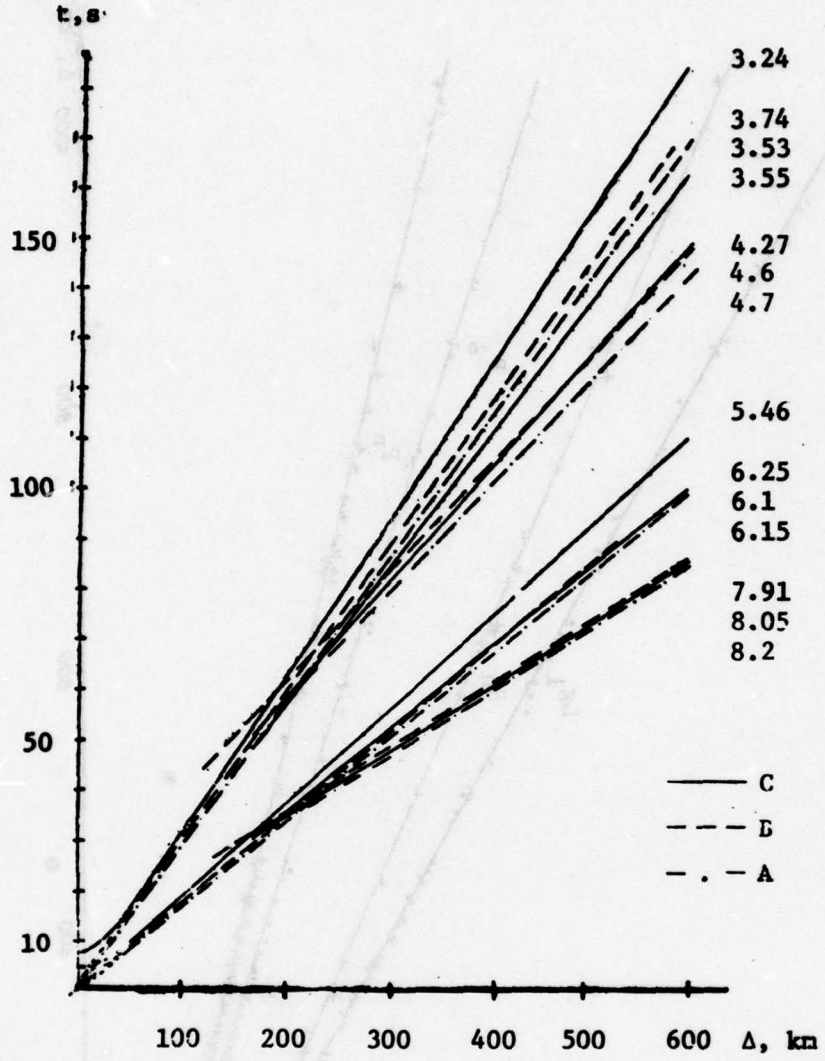

Fig. 16--Travel time curves of various body waves along the Chatkal range-Chuy-Ili valleys profile in Kirgizia determined by Medzhitova and Sabitova (A), Bune, et al. (B), and Rozova (C) [13]. Rozova's times are the standard times used in determining epicenters in Kirgizia.

The numbers on the right side are velocities in km/s

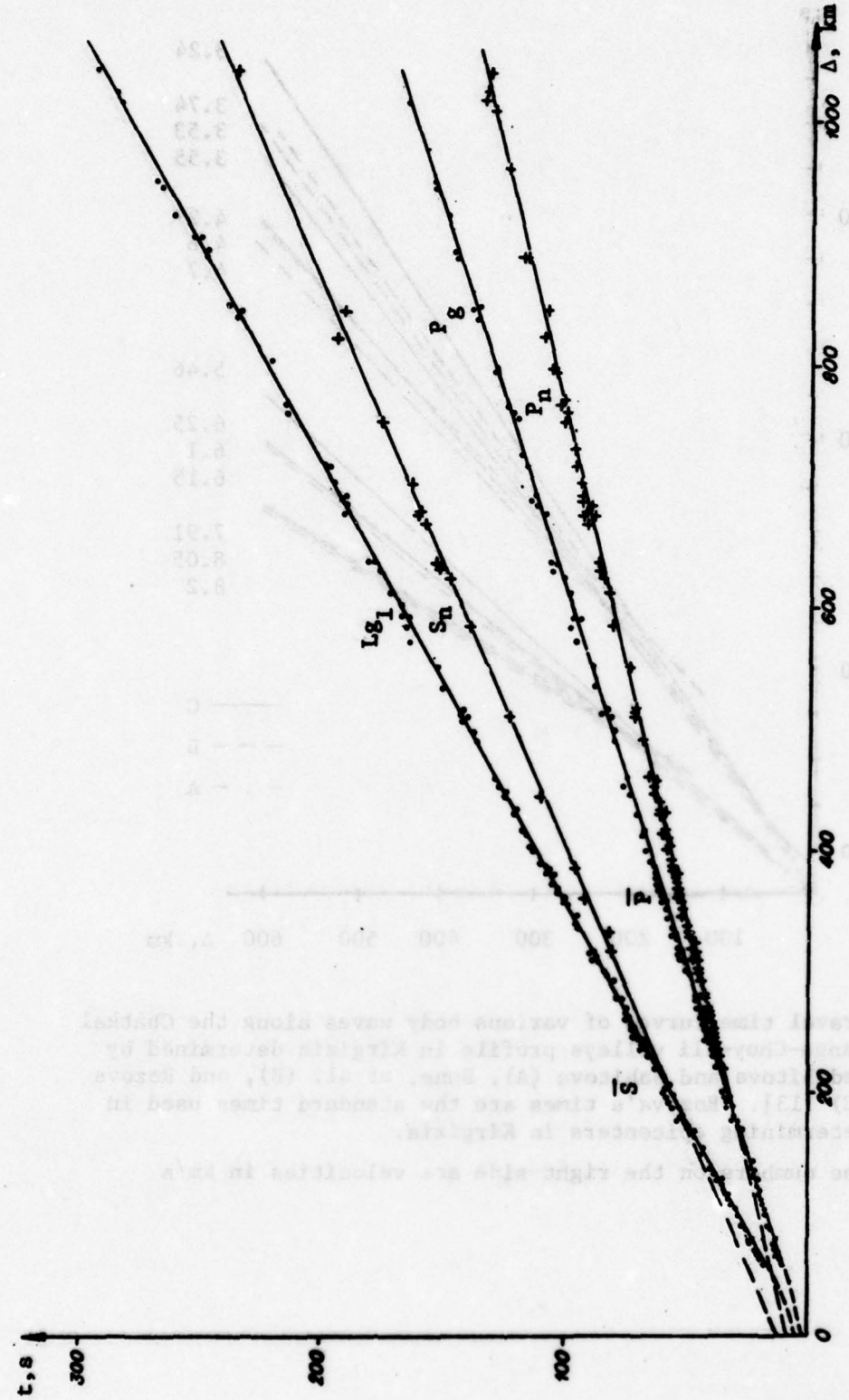

Fig. 17—Travel time curves of Lg and other phases for the Altay-Sayan region of Siberia [14]. The dots represent observation data. With a mean square error $\sigma_0 = 2$ s, the data on Lg can be approximated by a line given by the formula

$$t_{Lg} = t_0 + \frac{\Delta}{3.56 \pm 0.01}$$

Travel time curves of various phases including Lg_1 from a large chemical explosion and two local earthquakes in Soviet Central Asia (see footnote on pp. 22-23) are given in [9]. The travel time curves of all phases recorded from an unspecified large cratering explosion (m_b = 4.4 or 4.8) are shown in Fig. 18. Figure 19 shows travel time curves of body waves and the Lg phase from a shallow earthquake (No. 4 in Fig. 12) and Fig. 20 shows travel time curves for body waves and Lg from a crustal earthquake (No. 2) in Fig. 12.

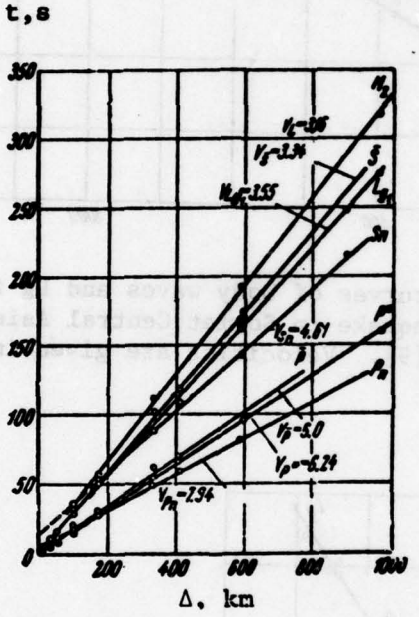

Fig. 18 --Travel time curves of body and surface waves including Lg_1 generated oy a chemical explosion somewhere in the area of Soviet Central Asia shown in Fig. 12. Velocities are given in km/s [9]

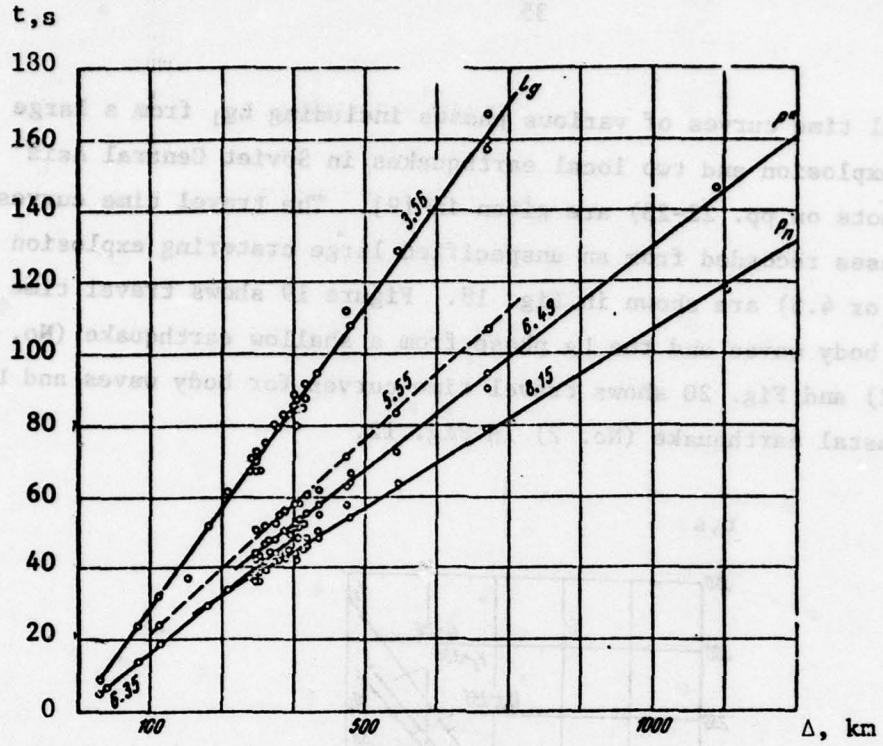

Fig. 19--Travel time curves of body waves and Lg from a crustal earthquake in Soviet Central Asia (No. 4 in Fig. 12) [9]. Velocities are given in km/s

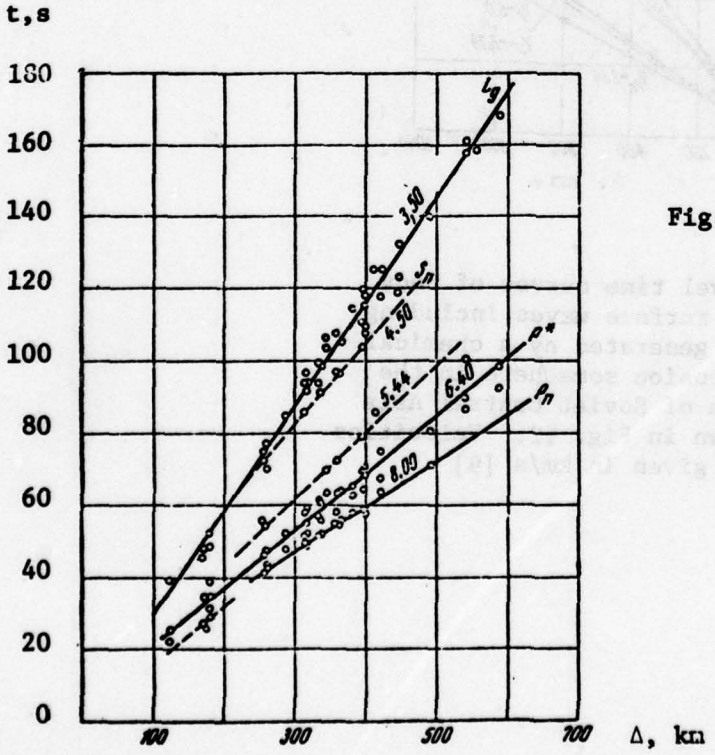

Fig. 20--Travel time curves of body waves and Lg from a crustal earthquake in Soviet Central Asia (No. 2 in Fig. 12) [9]. Velocities are given in km/s

VI. AMPLITUDE SPECTRA

The ChISS mean velocity amplitude spectra of $\overline{S}$ and Lg recorded at the Talgar station at four different epicentral distance ranges were published in a paper by Nurmagambetov [5]. The mean velocity amplitude spectra reduced to the energy class K = 10 were constructed using seismograms of earthquakes from four epicentral zones: vicinity of Talgar (Δ = 30 km), Chilik (Δ = 110 km), Khan-Tengri (Δ = 260 km) and Karakul' (Δ = 570 km). The velocity amplitude spectra of $\overline{S}$ and Lg recorded with the ChISS seismograph at the Talgar station at four different epicentral distances are shown in Fig. 21. It can be seen from this figure that at short epicentral distances the peak of the spectrum occurs at high frequencies (13 to 15 Hz). As the distance increases, the peak is gradually shifted toward lower frequencies and at Δ = 570 km it is found at 0.8 to 1.5 Hz. The decrease of the level of mean velocity amplitude spectra with distance is uneven and corresponds to that of the spectral amplitude distance curves shown in Fig. 10. The amplitude-curves in Fig. 10 can be used to interpolate spectra for epicentral distances between those shown in Fig. 21.

More detailed ChISS velocity amplitude spectra of Lg recorded at the Talgar and Vremennaya (temporary) stations (see Fig. 1a) at epicentral distances up to 2500 km, from earthquakes originating in epicentral zones in four different directions from Talgar and two different directions from Vremennaya, were published in the monograph by Antonova, et al. [6].

Figure 22 shows the velocity amplitude spectra of Lg for epicentral distances from 350 to 2500 km for different directions of propagation relative to the Talgar station. The spectra were normalized with respect to M = 5. Figure 23 shows analogous velocity amplitude spectra for Lg, constructed using the data acquired by the Vremennaya station, for two azimuthal directions, the first of which approximately coincides with the northwestern and eastern directions for the Talgar station and the second, with the western direction for the Talgar station. The velocity amplitude spectra of Lg for a fixed

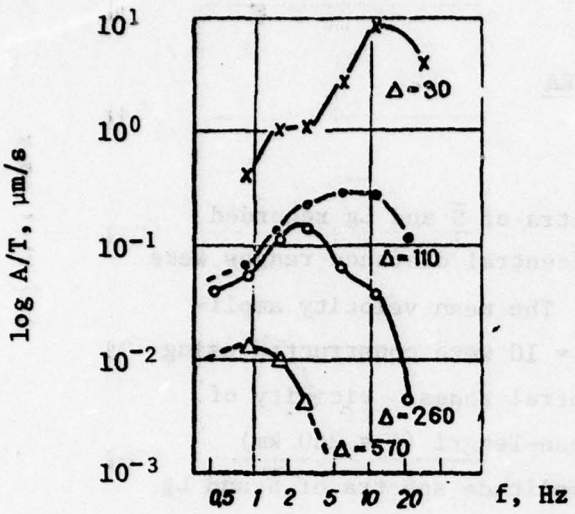

Fig. 21 --The ChISS velocity amplitude spectra of $\overline{S}$ and Lg recorded at the Talgar station, reduced to the energy class K = 10, for four different epicentral distances [5]. (The epicentral distance Δ is in km)

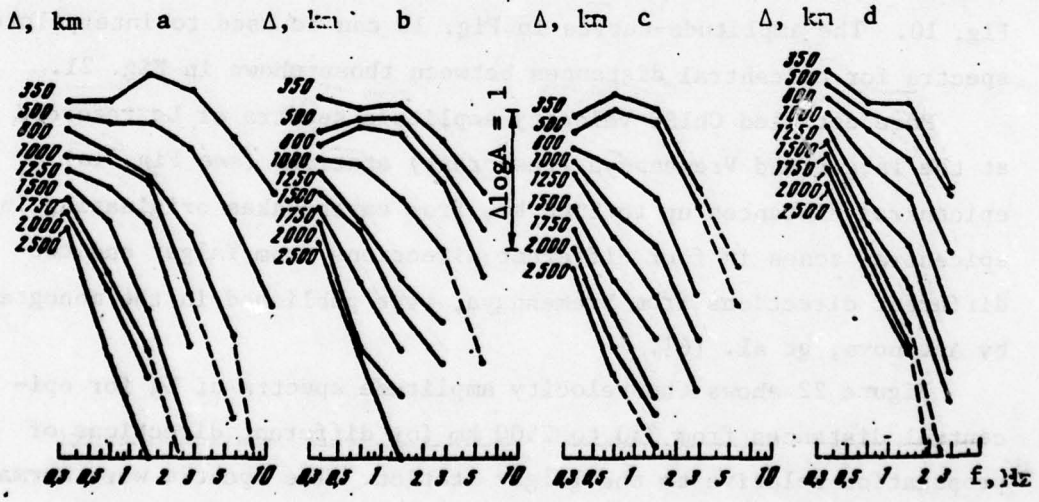

Fig. 22 --The velocity amplitude spectra of Lg phases recorded at the Talgar station for different epicentral distances for the northeastern (a), eastern (b), southern (c), and western (d) directions

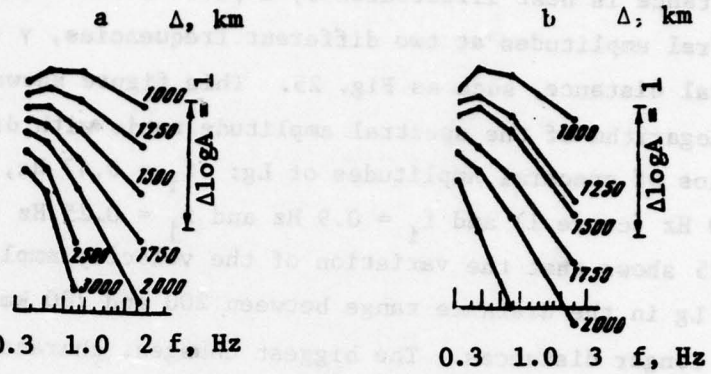

Fig. 23--The velocity amplitude spectra of Lg phases recorded at the temporary Vremennaya station for different epicentral distances for the eastern (a) and southwestern (b) directions

epicentral distance Δ = 300 km for the four different directions of propagation relative to the Talgar station are shown in Fig. 24. More detailed data on the spectral parameters of Lg in the four directions of propagation at a distance of 350 km and 800 km are given in Table 11. In this table, f_{max} denotes the position of ChISS spectral peaks and $\gamma\ (f_i/f_j)$ is the logarithm of the ratio of spectral amplitudes of Lg at frequencies f_i and f_j.

The differences in velocity amplitude spectra of Lg that are apparent at short distances are similar to the spectral differences of compressional waves. The velocity amplitude spectra in the northeastern direction have the highest frequency content. However, the low-frequency spectral component increases with increasing azimuth. For example, Table 11 shows that in the case Δ = 350 km the maximum differences between $\gamma\ (f_{0.7}\ /\ f_{2.8})$ reached 0.7 to 0.8 logarithmic unit and that the spectral peak in the northeastern and eastern directions is at 1.4 Hz, while in the western direction it lies below 0.35 Hz. In all but the southern direction, the velocity amplitude spectra at short distances are characterized by anomalously large amplitudes. The velocity amplitude spectra of Lg recorded at the Vremennaya station are characterized by higher-frequency content than those recorded at Talgar. However, the general behavior of the shape of the velocity amplitude spectra of Lg recorded at both stations is similar.

The variation of the shape of the velocity amplitude spectra with distance is best illustrated by a plot of the variation of ratios of spectral amplitudes at two different frequencies, γ (f_i/f_j), with epicentral distance, such as Fig. 25. This figure shows the variation of the logarithm of the spectral amplitude ratio with distance for two ratios of spectral amplitudes of Lg: f_i = 0.47 Hz, f_j = 0.9 Hz (curve 1) and f_i = 0.9 Hz and f_j = 0.25 Hz (curve 2). Figure 25 shows that the variation of the velocity amplitude spectrum of Lg in the distance range between 200 and 700 km is less than at longer distances. The biggest changes, characterized by stronger attenuation of higher frequencies, occur in the distance range between 600-800 km and 1300-1400 km. Oscillatory behavior, characterized by stronger attenuation of lower frequencies, occurs in the distance range 1300 to 1700 km. At distances exceeding 1500-2000 km, one can observe weaker regular variation in the shape of the velocity amplitude spectra with distance.

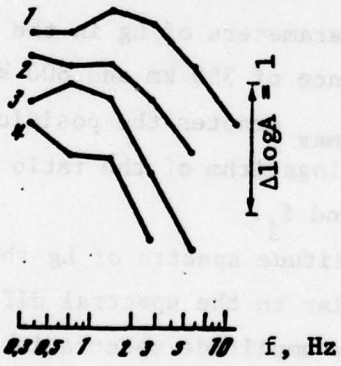

Fig. 24--The spectra of Lg at the epicentral distance Δ = 300 km for the northeastern (1), eastern (2), southern (3) and western (4) directions of propagation

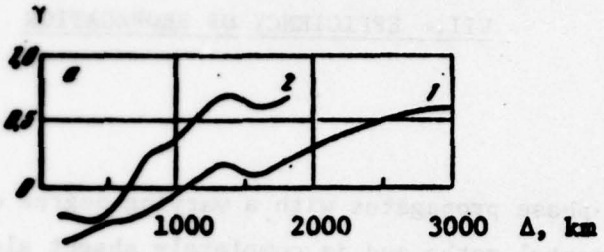

Fig. 25--A plot of $\gamma\ (f_{0.47}/f_{0.9})$ and $\gamma\ (f_{0.9}/f_{0.25})$ vs distance, curves 1 and 2, respectively, where $\gamma\ (f_i/f_j)$ is the logarithm of the ratio of spectral amplitudes at frequencies f_i and f_j. Based on the seismograms of a ChISS system at the Vremennaya station

Table 11 [6]

SPECTRAL PARAMETERS OF Lg IN FOUR DIRECTIONS OF PROPAGATION

Parameter	NE		E		S		W	
	350	800	350	800	350	800	350	800
f_{max}	1.4	0.35	1.4	0.7	0.7	<0.35	<0.35	<0.35
γ(0.35/0.7)	0	0.17	0.07	0.12	0.17	0.13	0.23	0.23
γ(0.7/2.8)	-0.10	0.60	0.23	0.40	0.65	0.92	0.62	0.77
γ(1.4/5.6)	0.47	1.15	0.65	1.07	1.10	-	-	-

VII. EFFICIENCY OF PROPAGATION

A. GENERAL

The Lg phase propagates with a varying degree of efficiency along continental paths and is completely absent along oceanic paths. The most efficient propagation occurs across stable shield and platform regions with a relatively homogeneous, high-Q crust, such as the Siberian and Kazakh platforms, Indian shield, etc. It has been suggested that the efficiency of propagation of Lg depends on the presence of the granitic layer: very efficient when its thickness is normal, less efficient when it is thin and completely absent when the granitic layer is absent. Thus, the efficiency of propagation of Lg can be used to map regions with crustal structure differing from those of adjacent areas. Soviet scientists have investigated efficiency of propagation across both oceanic and crustal structures [6,8,11,15-25]. It was determined that in continental areas the Lg is not propagated across the central part of the Black Sea [11,18-22], the Tibetan plateau [6,8,23,24] and the central and southern parts of the Caspian Sea [18,19].

B. EFFICIENCY OF PROPAGATION OF Lg ACROSS THE BLACK SEA

The efficiency of propagation of Lg across the Black Sea Basin was investigated in [22] using seismograms of 60 crustal earthquakes with surface wave magnitude M = 4 to 5.5 originating during 1950-1968. The earthquakes were recorded by three Caucasian seismographic stations (Tbilisi, Erevan, Sochi), two Crimean stations (Simferopol', Yalta) (see Fig. 1a), two Bulgarian stations (Sofia, Dimitrograd) and three Turkish stations. The efficiency of propagation of Lg was investigated by examining seismograms to see if Lg is strong, weak, or absent and plotting these three types of paths on the map. In Fig. 26 continuous lines denote propagation paths of strong Lg and Rg; dot-dashed lines, weak Lg and Rg and broken lines denote paths characterized by the absence of Lg and Rg. It can be seen from this figure that without exception Lg and Rg are absent when the path traverses the central part of the Black Sea basin. This is clearly

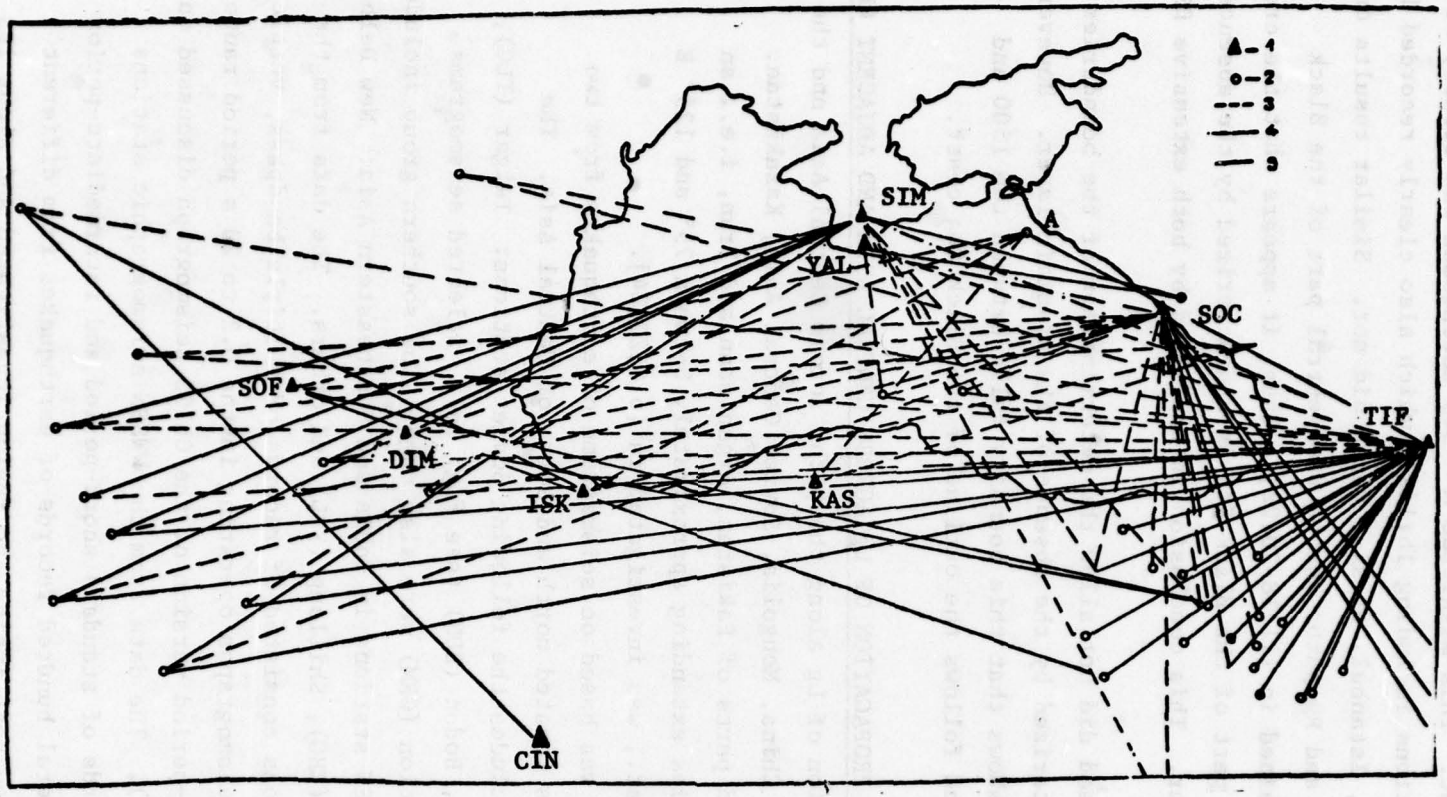

Fig. 26--Propagation paths of Lg and Rg across the Black Sea Basin [21]
1--Seismographic station
2--Earthquake epicenters
3--Propagation paths characterized by the absence of Lg and Rg
4--Propagation paths characterized by weak Lg and Rg
5--Propagation paths characterized by strong Lg and Rg
A--Anapa earthquake of 12 July 1966

demonstrated by the 12 July 1966 Anapa earthquake (A in Fig. 26) originating in the crust. This magnitude M = 5.5 earthquake was clearly recorded by all stations including Tbilisi, which also clearly recorded Lg and Rg, and Sofia, Istanbul, et al., which did not. Similar results on the absence of Lg and Rg paths across the central part of the Black Sea were also obtained in [11,18-20,22]. Thus, it appears that the crust under the central part of the Black Sea is characterized by the absence of a granitic layer. This conclusion is confirmed by both extensive DSS and gravity data.

The method used did not allow the determination of the boundaries of the region characterized by the absence of the granitic layer. However, a rough estimate shows that this boundary falls between the 1500 and 2000 m isobaths and follows the outline of the Black Sea coast.

C. EFFICIENCY OF PROPAGATION OF Lg ACROSS CENTRAL ASIA AND ADJACENT REGIONS

The propagation of Lg along the paths across Central Asia and the adjacent areas in China, Mongolia, Soviet Central Asia, Kazakhstan, Siberia, India and parts of Pakistan, Afganistan and Iran, i.e., an area with boundaries extending approximately between 75° and 125° E Long. and 20° N Lat., was investigated in [6,8,23,24].

The analysis was based on seismograms of earthquakes from two groups of stations located north and south of Central Asia. The northern group includes the following Soviet stations: Talgar (TLG), Novosibirsk (NSB), Bodon (BDN) (see Fig. 1a). Selected seismograms from the Garm station (GRM) were also used. The southern group included the following WWSSN stations in India and Southeastern Asia: New Delhi (NDI), Chiengmai (CHG), Shillong (SHL) and others. The data from the four Soviet stations consisted of records of multiple bandpass, vertical-component ChISS seismographs operating in the 0.2 to 20 s period range (modified, longer-period version of the ChISS seismograph discussed on p. 1 of this note). The data from the WWSSN seismographic stations consisted of records of standard short-period and intermediate-period instruments. Several hundred records of earthquakes from different focal zones located both inside the region investigated and along its boundaries were used in the analysis. Most of the magnitudes of

earthquakes utilized were between 4.5 and 5.5 The epicentral distances varied between 300 km and 3000 and 3500 km.

The efficiency of propagation of Lg was investigated by examining the seismograms to see if Lg is strong, weak (amplitude of Lg approximately equal to or somewhat weaker than that of P), or absent. The epicenters of these three groups of earthquakes were plotted on a map. Four such maps of earthquakes recorded at the Talgar, Vremennaya, Novosibirsk and Bodon stations are shown in Figs. 27, 28, 29 and 30, respectively.

Analysis of the data shown in Figs. 27 through 30 shows that Lg propagates efficiently across the Eurasian platform and across the Indian Shield. The Lg phase is also recorded with large amplitudes at Talgar and Novosibirsk when the paths between the station and the earthquakes originating in the Kunlun and Altyn Tagh cross the Tarim basin. However, the signals are less sharp than the signals propagating along paths crossing only the Indian Shield or the Siberian Platform. As the paths that cross the Tarim basin also cross the Tien Shan, the less sharp signals can be attributed to the variation in structure beneath the Tien Shan. Lg also propagates efficiently across another large stable area, southwest China.

The propagation of Lg across the Tien Shan is less efficient when paths are more oblique to the trend of the range than when they are perpendicular to it. Earthquakes in the eastern Tien Shan radiate clear Lg phases to stations in Novosibirsk and Bodon, but at Talgar, Lg is often very weak. The differences in the signals may be partially attributed to the different amounts of the paths in the more complicated structure of the Tien Shan.

In contrast, Lg was completely absent for paths across the Tibetan plateau. Since Lg from the same earthquakes propagating along paths which do not cross Tibet were generally recorded (see Figs. 30 and 31), the absence of Lg can be attributed to Tibet or its margin and not the sources. This is clearly illustrated by Fig. 33, which shows amplitude-distance curves of Lg propagating along two different directions (Baykal and Tibet), recorded at the Talgar and Vremennaya

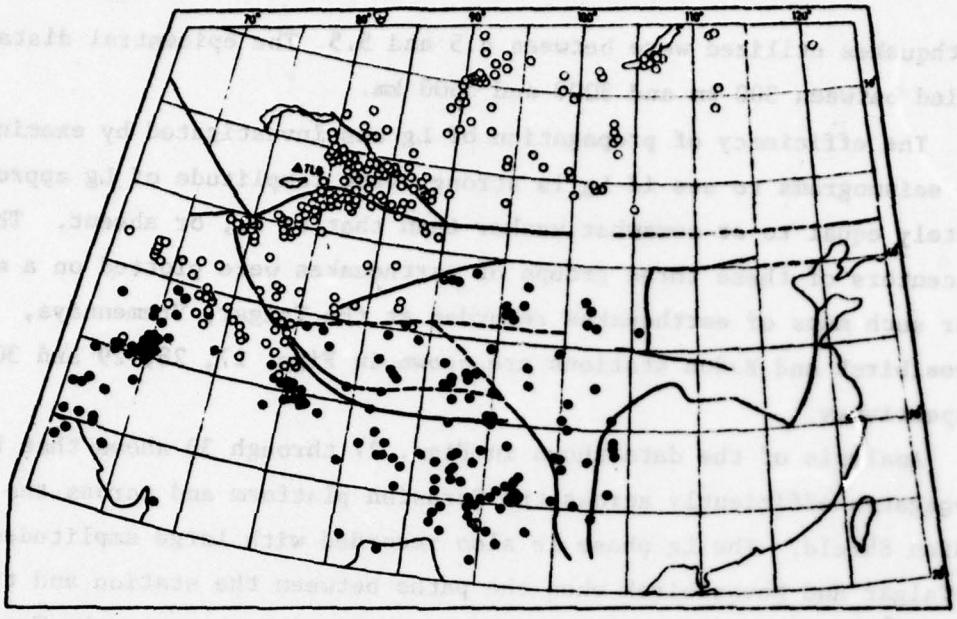

Fig. 27--Epicenters of earthquakes recorded at the Talgar station classified according to whether Lg on the seismograms acquired with the multiple-bandpass ChISS seismograph system is clear, weak or absent [8,24]

- o Lg clear
- ⊖ Lg weak
- ● Lg absent
- ___ large faults

stations. It can be seen from this figure that at epicentral distances corresponding to the northern boundary of the Tibetan plateau the amplitudes of Lg propagating in the Tibet direction diminish by an order of magnitude in comparison with the amplitudes of Lg propagating in the Baykal direction. Since in determining the amplitude curves in Fig. 33 when the Lg phase was absent the authors measured the amplitudes of phases within the sector of the seismogram where Lg should have been recorded, the actual decrease in amplitudes of Lg along the Tibetan plateau direction was much greater than that shown in Fig. 33. It is interesting to note that the Baykal rift zone has no effect on the efficiency of propagation of Lg across this structure.

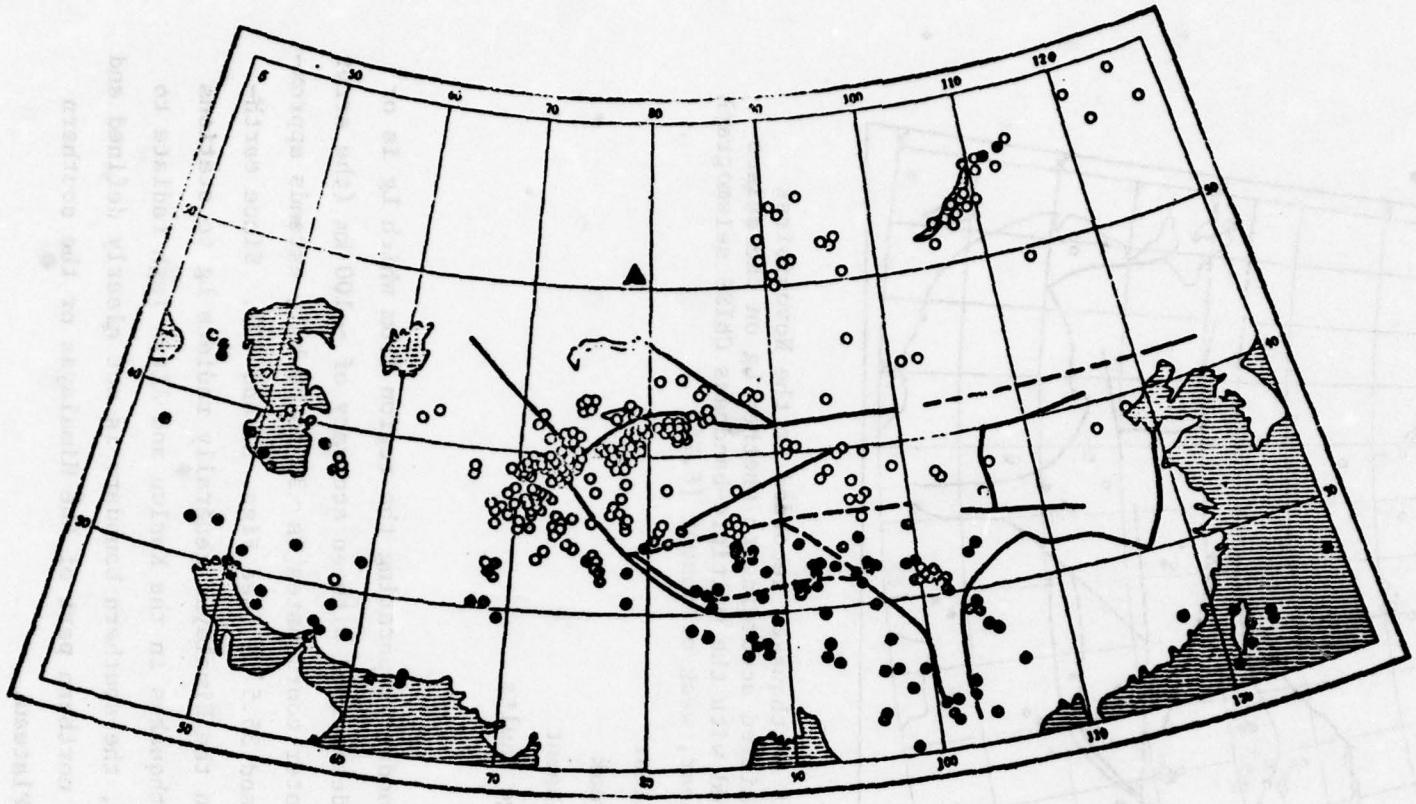

Fig. 28 --Epicenters of earthquakes recorded at the Vremennaya station classified according to whether Lg on the seismograms acquired with the multiple-bandpass ChISS seismograph system is clear, weak or absent [8,22]

- o Lg clear
- ⊙ Lg weak
- ● Lg absent
- ═══ large faults
- ▲ Vremennaya station

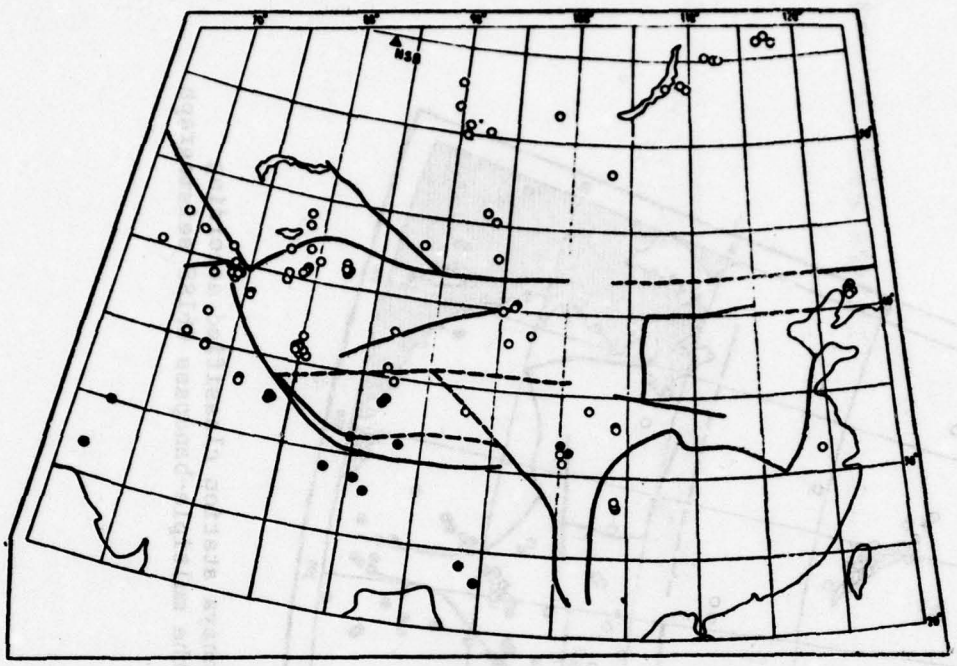

Fig. 29--Epicenters of earthquakes recorded at the Novosibirsk station classified according to whether Lg on the seismograms acquired with the multiple-bandpass ChISS seismograph system is clear, weak or absent [8,24]

- o Lg clear
- ⊙ Lg weak
- ● Lg absent
- ——— large faults
- - - -

The northern boundary separating the region from which Lg is or is not transmitted, determined with an accuracy of ~ 100 km (the error of determining epicenter coordinates is ~30 to 50 km), extends approximately between 34° and 35.5° N (see Figs. 31 and 32). Since earthquakes originating in the Himalayas generally radiate Lg to stations in India and the earthquakes in the Kunlun and Altyn Tagh radiate to stations in the USSR, the southern boundary is not clearly defined and appears to be in the northern part of the Himalayas or the southern part of the Tibetan Plateau.

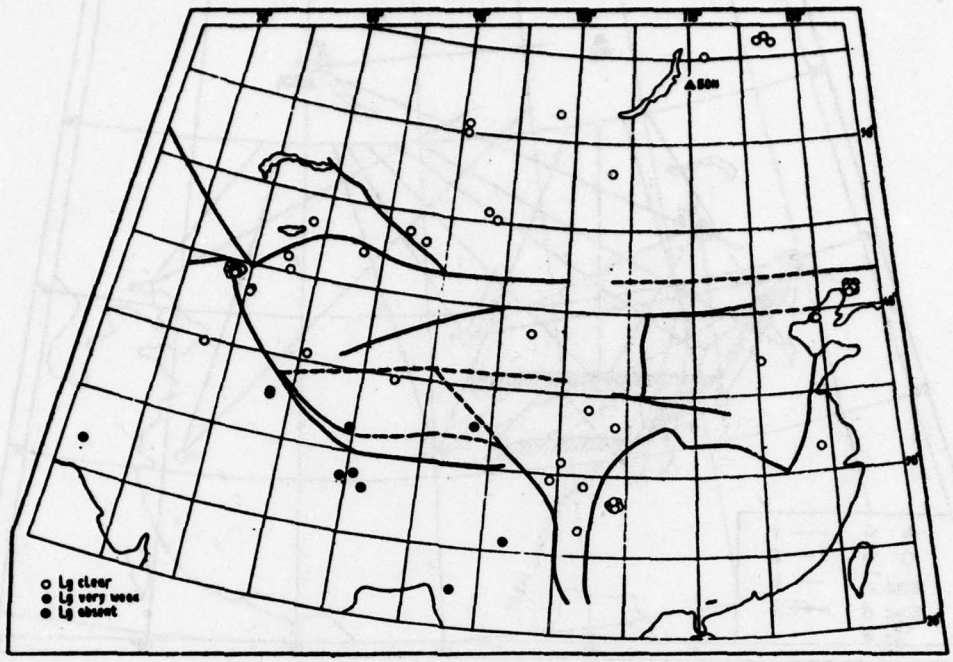

Fig. 30--Epicenters of earthquakes recorded at the Bodon station classified according to whether Lg on the seismograms acquired with the multiple-bandbass ChISS seismograph system is clear, weak or absent [8,24]

- o Lg clear
- ⊖ Lg weak
- ● Lg absent
- ___ large faults

Weak boundaries causing a decrease in the amplitudes of Lg can also be identified. For example, a weak boundary (see Figs. 31 and 32) extends along the Hindu-Kush-Karakorum arc and its southeastern extension. Weak boundaries also coincide with the Cis-Kopet-Dag downwarp and, further to the east, with the Gerat fault and the northwestern margin of the Indian shield.

In summary, Lg is reliably recorded in all parts of the Asian continent north of the Kopet-Dag and its extensions, north of the Tibetan plateau and within the Indian shield. The Lg phases are attenuated when crossing Pamir-Hindu-Kush and Tien Shan and especially when the path extends along the Tien Shan and the Himalayas. The Lg

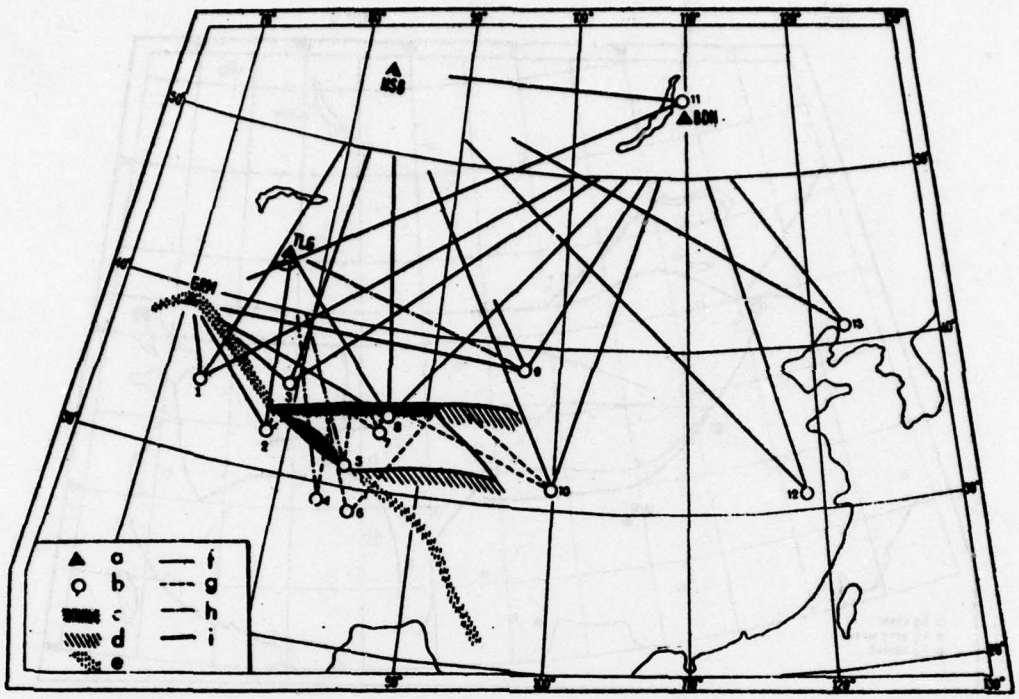

Fig. 31--Map showing interpretation of selected paths to northern stations [8,24]

a--seismographic stations
b--epicenters
c--apparent sharp boundaries of Lg propagation
d--less sharp boundaries
e--presumed southern boundary
f--clear Lg
g--no Lg
h--weak Lg
i--large faults

phases disappear when generated by earthquakes located within the Tibetan plateau or when the path even partially crosses this region (100 to 150 km of the path along Tibet is sufficient for the Lg phases to disappear completely).

While the amplitudes of Lg decrease when crossing the boundary of the Tibetan plateau, the shape of the spectra of Lg hardly changes at all. Thus, it appears unlikely that the disappearance of Lg when the path crosses the Tibetan plateau can be attributed to attenuation. Since Lg is known to propagate efficiently in areas characterized by sharp changes in the crustal thickness and composition of the crust

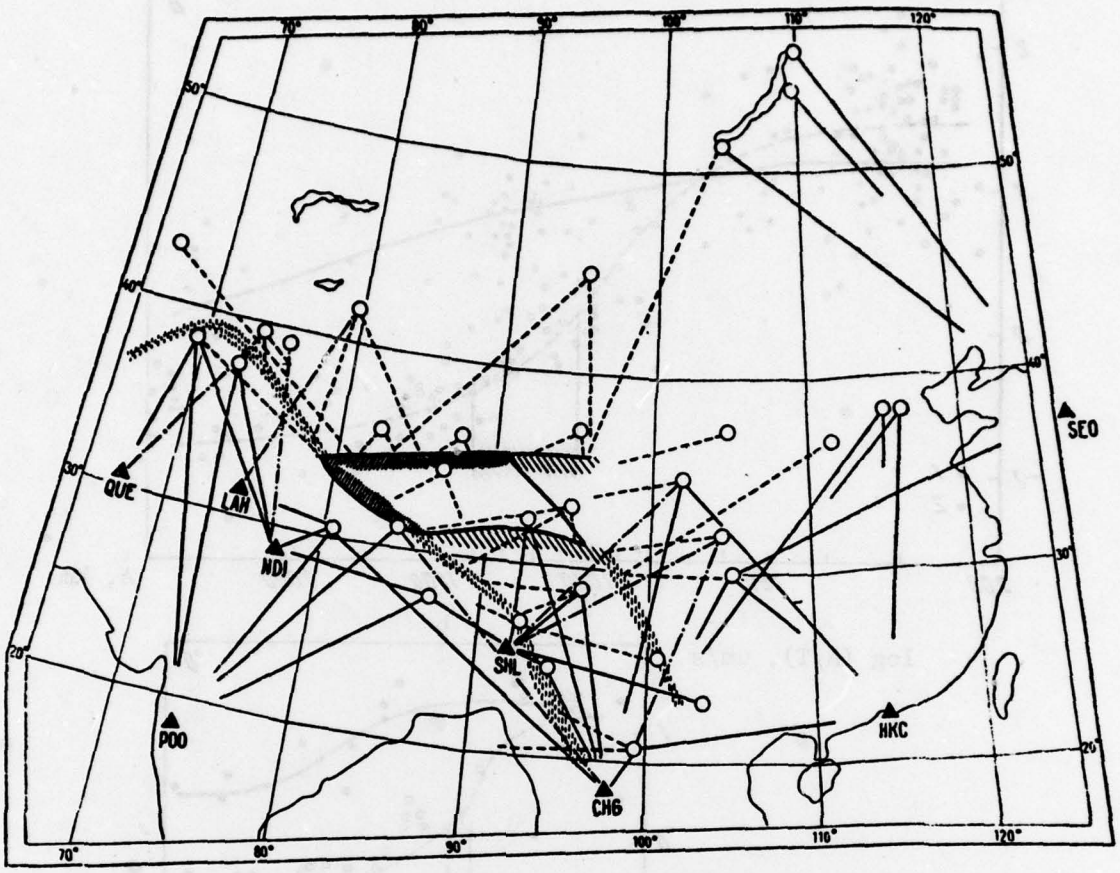

Fig. 32--Map showing interpretation of selected paths to southern stations: triangles, stations; circles, epicenters; dense hatching, apparent sharp boundaries of Lg propagation; open hatching, less sharp boundaries; dashed hatching, presumed southern boundary; solid line, clear Lg; dashed line, no Lg; dotted-dashed line, weak Lg; and heavy dark line, large faults [8,24]

(Pamir-Tadzhik basin, Hindu-Kush-Badakhsh basin, etc.), a sharp change in crustal thickness appears to be also unlikely to cause disappearance of Lg. Therefore, the absence or wedging out of the granitic layer is probably the cause of absence of Lg when the path crosses at least a sector of the Tibetan plateau.

The efficiency of propagation of Lg across Central Asia and adjacent regions was also investigated in [25] using seismograms from as many as 54 seismographic stations along the 3500-km-long Pamir-Lena River profile (A-A' in Fig. 1a). Efficiency of propagation was investigated

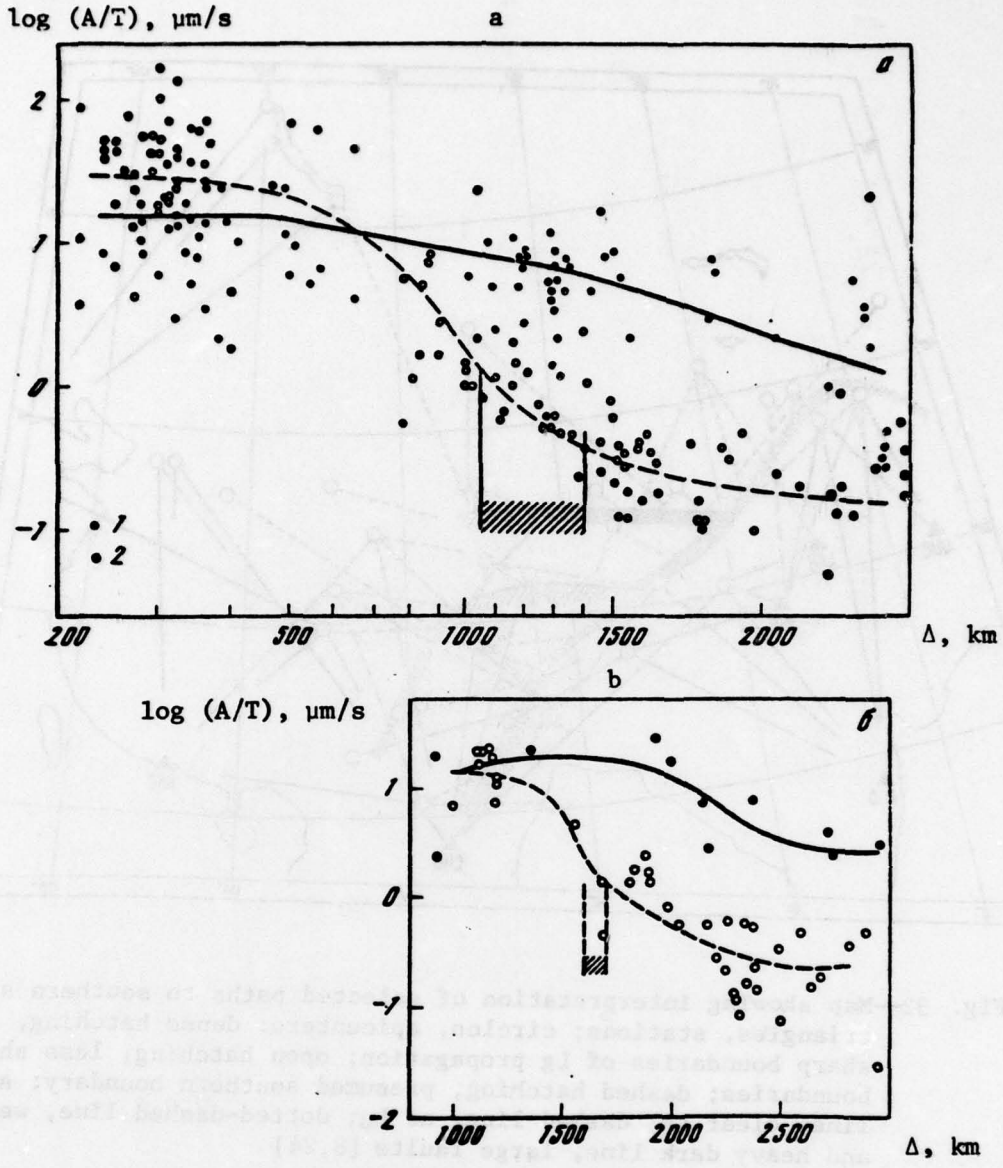

Fig. 33--Amplitude-distance (attenuation) curves of Lg recorded by the Talgar (a) and Vremennaya (b) seismographic stations [6]

—— Baykal direction, -----Tibet direction

The hatched area denotes the epicentral distance range corresponding to the boundary of the Tibetan plateau

along paths from earthquakes to the stations crossing large structures of interest. The results obtained were plotted in terms of the amplitude ratios A_{Lg}/A_P recorded by the stations along the profile. Figures 34 through 38 show plots of A_{Lg}/A_P from epicentral regions in Cisbaykal, Sinkiang province, Gobi desert, Southwest China and Himalayas. Each figure includes a map of the area showing epicenters, locations of stations along the profile and the important structural features of the region. From Figures 34 through 38 it can be seen that the amplitudes of Lg decrease 3 to 7 times along the paths across Altay, 6 to 8 times across the Himalayas and 10 times across Tibet. However, these conclusions were reached on the basis of analysis of a small number of earthquakes.

D. EFFICIENCY OF PROPAGATION OF Lg ACROSS THE CASPIAN SEA

The efficiency of propagation of Lg and Rg across the Caucasus and adjacent areas was investigated in [18] using seismograms of 58 earthquakes with surface wave magnitudes $M \geq 4$, originating during 1950-1960 at epicentral distances Δ = 600 to 6000 km. The earthquakes were recorded with three-component, broadband SK seismographs at the Tbilisi station (41°43'N, 44°48'E). The efficiency of propagation of these phases was investigated by examining the seismograms to see if Lg and Rg are present or absent and plotting these two types of paths on a map. In Fig. 39, continuous lines denote efficient propagation paths of Lg and Rg and dashed lines denote paths characterized by their absence. From this figure it can be seen that the Lg and Rg from 14 earthquakes traversing the southern and central parts of the Caspian Sea Basin are not recorded, while these phases from three earthquakes, traversing the northern part of the Caspian Sea Basin are recorded. Similar results were also obtained in [19] using the same technique on numerous earthquakes originating in 1960 to 1961 at Δ = 400 to 600 km and recorded at the Tbilisi, Simferopol', Sochi and Erevan seismographic stations.

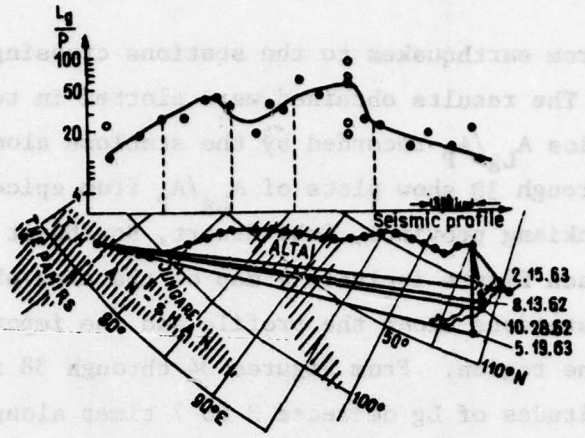

Fig. 34--Relative amplitude-distance, i.e., A_{Lg}/A_P, curves for seismic waves generated by four earthquakes originating in the Cisbaykal region and recorded by seismographic stations along the Pamir-Lena River profile [25]

● - recorded by short-period SKM-3 seismograms

o - recorded by unspecific long-period (probably SKD) seismograms

/// - mountain chain

The date identifies the earthquake. A few straight lines show the path from the earthquakes to the seismographic stations

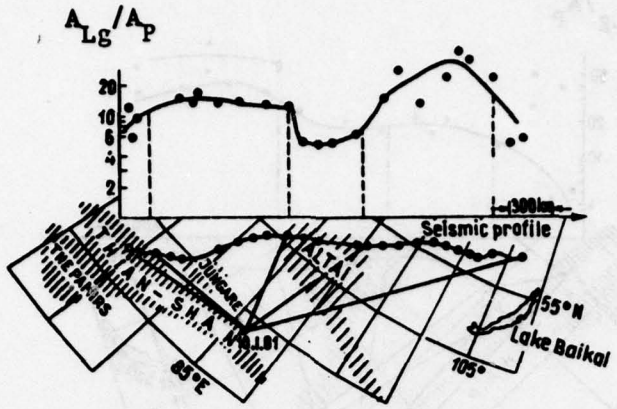

Fig. 35--Relative amplitude-distance, i.e., A_{Lg}/A_P, curves for seismic waves generated by four earthquakes originating in the Sinkiang province and recorded by seismographic stations along the Pamir-Lena River profile [25]

- ● - recorded by short-period SKM-3 seismograms
- o - recorded by unspecified long-period (probably SKD) seismograms
- /// - mountain chain

The date identifies the earthquake. A few straight lines show the paths from the earthquakes to the seismographic stations

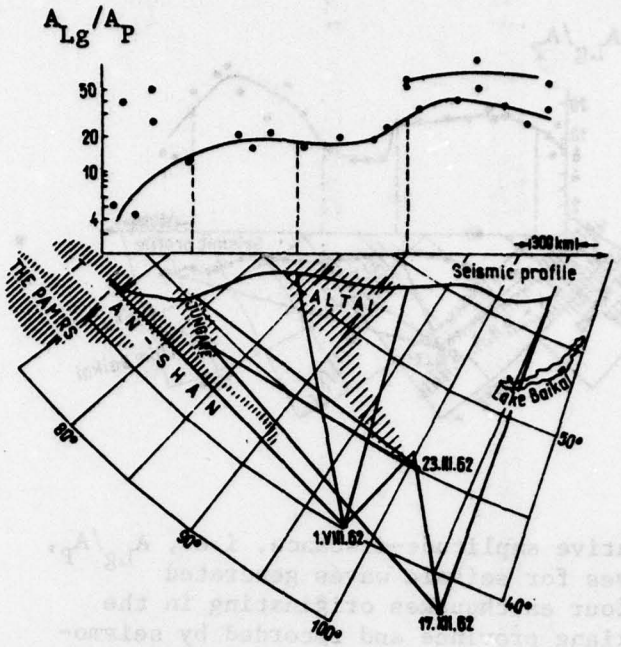

Fig. 36--Relative amplitude-distance, i.e., A_{Lg}/A_P, curves for seismic waves generated by four earthquakes originating in the Gobi desert and recorded by seismographic stations along the Pamir-Lena River profile [25]

● - recorded by short-period SKM-3 seismograms

o - recorded by unspecified long-period (probably SKD) seismographs

///- mountain chain

The date identifies the earthquake. A few straight lines show the paths from the earthquakes to the seismographic station

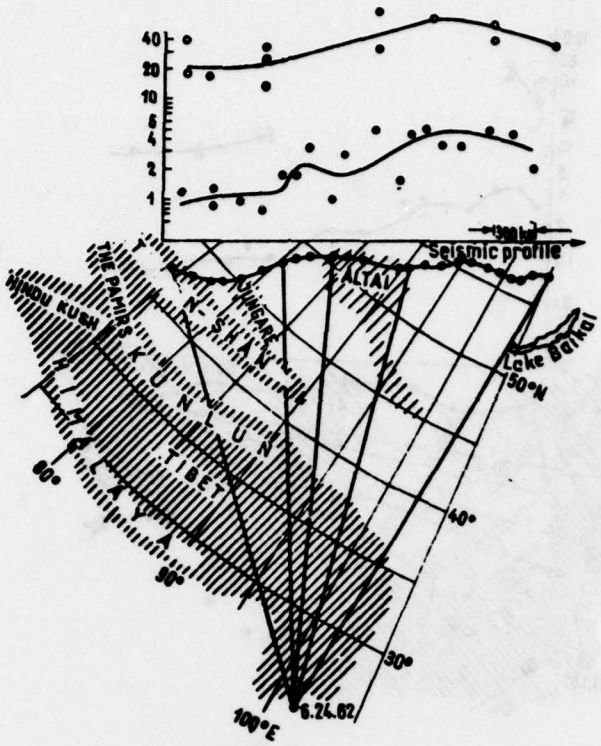

Fig. 37--Relative amplitude-distance, i.e., A_{Lg}/A_P, curves for seismic waves generated by four earthquakes originating in South West China and recorded by seismographic stations along the Pamir-Lena River profile [25]

● - recorded by short-period SKM-3 seismograms

o - recorded by unspecified long-period (probably SKD) seismograms

/// - mountain chain

The date identifies the earthquake. A few straight lines show the paths from the earthquakes to the seismographic stations

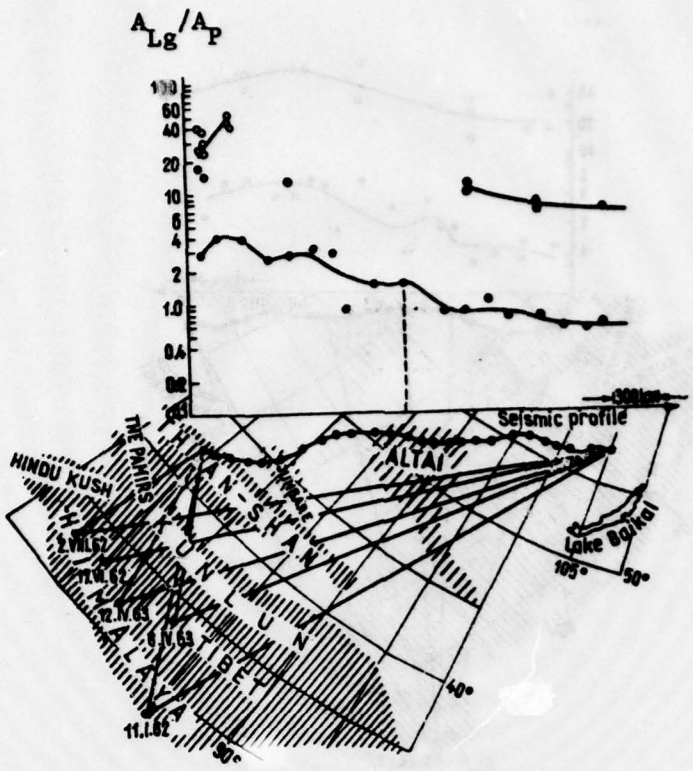

Fig. 38--Relative amplitude-distance, i.e., A_{Lg}/A_P, curves for seismic waves generated by four earthquakes originating in the Himalayas and recorded by seismographic stations along the Pamir-Lena River profile [25]

• - recorded by short-period SKM-3 seismographs

o - recorded by unspecific long-period (probably SKD) seismographs

/// - mountain chain

The date identifies the earthquake. A few straight lines show the paths from the earthquakes to the seismographic station

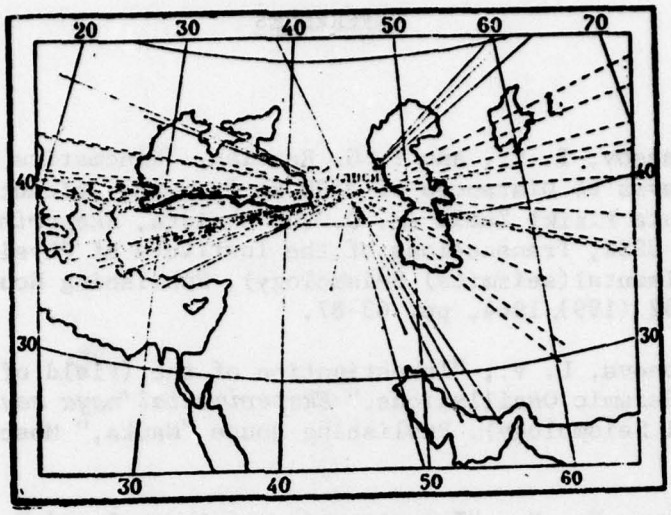

Fig. 39--Propagation paths of Lg and Rg across the Caspian Sea Basin [18]

———— Propagation paths characterized by the presence of Lg and Rg

-------- Propagation paths characterized by the absence of Lg and Rg

REFERENCES

1. Nersesov, I. L., and T. G. Rautian, "Kinematics and Dynamics of Seismic Waves to Distances of 3500 km from the Epicenter," AN SSR, Trudy Instituta Fiziki Zemli im. O. Yu. Shmidta, *Eksperimental'naya seismika* (AS USSR, Transactions of the Institute of Physics of the Earth, Experimental(seismics) Seismology), Publishing House "Nauka," Moscow, No. 32 (199), 1964, pp. 63-87.

2. Antonova, L. V., "Investigation of the (Field of) Dynamic Features of Seismic Oscillations," *Eksperimental'naya seysmologiya* (Experimental Seismology), Publishing House "Nauka," Moscow, 1971, pp. 107-112.

3. Sedova, Ye. N., "Investigation of Crustal and Upper Mantle Inhomogeneities From the Dynamic Characteristics of Distant Earthquakes," *Eksperimental'naya seysmologiya* (Experimental Seismology), Publishing House "Nauka," Moscow, 1971, pp. 97-107.

4. Khalturin, V. I., "Seismic Wave Absorption in the Crust of Tien Shan," *Eksperimental'naya seysmologiya* (Experimental Seismology), Publishing House "Nauka," Moscow, 1971, pp. 125-136.

5. Nurmagambetov, A., "Attenuation of Seismic Waves and Energy Classification of Earthquakes From Observations Acquired with ChISS Seismographic Systems," *Magnituda i energicheskaya klassifikatsiya zemletryaseniy* (Magnitude and Energy Classification of Earthquakes), Vol. 2, Moscow, 1974, pp. 164-173.

6. Antonova, L.V., F. F. Aptikayev, R. I. Kurochkina, I. L. Nersesov, A. V. Nikolayev, A. I. Ruzaykin, Ye. N. Sedova, A. V. Sitnikov, F. S. Tregub, L. D. Fedorskaya and V. I. Khalturin, *Eksperimental'nyye seysmicheskiye issledovaniya nedr zemli* (Experimental Seismic Investigations of the Earth's Interior), AN SSR, Institut fiziki zemli im. O. Yu. Schmidta (AS USSR, Institute of Physics of the Earth), Publishing House "Nauka," Moscow, 1978, 155 pages, (Chapter 2).

7. Khalturin, V. I., T. G. Rautian, A Nurmagambetov, V. L. Golubyatnikov, Ye. E. Blagoveshchenskaya and T. F. Belikova," Dependence of Spectra of Seismic Oscillations on the Energy of Earthquakes," *Voprosy kolichestvennoy otsenki seismicheskoy opasnosti* (Quantitative Evaluation of Seismic Danger), Publishing House "Nauka," Moscow, 1975, pp. 123-129.

8. Molnar, P., I. L. Nersesov, A. I. Ruzaikin, and V. I. Khalturin, "Lg Waves and Their Propagation in Central Asia," *Sbornik sovetoamerikanskikh rabot po prognozu zemletryaseniy* (Collection of Articles on Soviet-U.S. Investigations on Earthquake Prediction), Publishing House "Donish," Dushambe-Moscow, 1976, Vol. 1, pp. 185-206.

9. Pasechnik, I. P., *"Kharakteristika seysmicheskikh voln pri yadernykh vzryvakh i zemletyaseniyakh,"* (Characteristics of Seismic Waves from Nuclear Explosions and Earthquakes), Publishing House "Nauka," Moscow, 1970.

10. Pataraya, Ye. I., "Travel Time Curves of Lg and Rg for Epicentral Distances Between 200 and 1500 km," *Informatsionniy byulletin' ESSN* (Information Bulletin of the Unified Seismic Observation System), No. 9, 1963, (Quoted in [11]).

11. Mindeli, P. Sh., Yu. P. Neprochnov and Ye. I. Pataraya, "Determination of the Region Characterized by the Absence of the Granitic Layer in the Black Sea Basin, from DSS and Seismological Data," *AN SSSR, Izvestiya, Seriya geologicheskaya,* No. 2, 1965, pp. 7-15.

12. Val'dner, N. G., "Travel Time of L_1, Lg_1, Lg_2 and Rg," *AN SSSR, Izvestiya, Seriya geofizicheskaya,* No. 6, 1961, pp. 882-888.

13. Medzhitova, Z. A. and T. M. Sabitova, "Investigation of Seismic Velocities and the Crustal Structure of the Chuy Valley and of Adjacent Regions," Chapter 3, Section 1, in a book by O. K. Chidiya and T. M. Sabitova, editors, *Opyt Kompleksnogo seysmicheskogo rayonirovaniya na primere Chuyskoy vpadini* (Experience Gained in Seismic Regionalization Using the Chuy Valley as an Example), Frunze, 1975, pp. 46-65.

14. Tsibul'chik, G. M., "Travel Time Curves of Seismic Phases and the Crustal Structure of the Altay-Sayan Region," a chapter in a book by V. N. Gayskiy, et al., editors, *Regional'nyye geofizicheskiye Issledovaniya v Sibiri* (Regional Geophysical Investigations in Siberia), Novosibirsk, 1967, pp. 159-169.

15. Val'dner, N. G. and Ye. F. Savarenskiy, "On the Nature of Lg Phase and Its Propagation in Northeastern Asia," *AN SSSR, Izvestiya, Seriya geofizicheskaya,* No. 1, 1961, pp. 3-24.

16. Koridalin, Ye. A., "Certain Features of Lg and Rg Phases and Regional Characteristics of Their Propagation," *AN SSSR, Izvestiya, Seriya geofizicheskaya,* No. 8, 1961, pp. 1114-1121.

17. Pshennikov, K. V., "Lg Waves from Observations in Irkutsk," *Geologiya i geofizika,* No. 5, 1961, pp. 87-90.

18. Sikharulidzhe, D. I., "The Nature of Lg and Rg and the Investigation of the Structure of the Earth's Crust," *AN Gruz SSR, Trudy Instituta Geofiziki* (AS Georgian SSR, Transactions of the Geophysical Institute), Vol. 22., 1963 (1964), pp. 57-70.

19. Sikharulidze, D. I., Ye. I. Pataraya and V. G. Padalashvili, "Crustal Studies Using Data on Propagation of Short-Period Surface Waves," *AN Gruz SSR, Trudy Instituta Geofiziki* (AS Georgian SSR, Transactions of the Geophysical Institute), Vol. 22, 1963 (1964), pp. 71-84.

20. Savarenskiy, Ye. F., and N. G. Val'dner, "Lg and Rg Phases from Earthquakes in the Black Sea Basin and Certain Ideas Concerning their Nature," *Seismicheskiye issledovaniya* (Seismic Investigations), Moscow, Publishing House AN SSSR, No. 4, 1960, pp. 55-77.

21. Balavadze, B. K., and P. Sh. Mindeli, "Crustal Structure of the Black Sea Basin from Geophysical Data," *Seismicheskiye Issledovaniya* (Seismic Investigations), Moscow, Publishing House "Nauka", No. 6, 1965, pp. 66-76.

22. Mindeli, P. Sh., and Ye. I. Pataraya, "Results of the Investigations of Propagation of Short-Period Seismic Surface Waves in the Black Sea Basin," *AN Gruz SSR, Trudy Instituta Geofiziki* (AS Georgian SSR, Transactions of the Geophysical Institute), Vol. 29, 1972, pp. 34-41.

23. Molnar, P., I. L. Nersesov, A. I. Ruzaykin and V. I. Khalturin, "Variation of Dynamic Properties of Lg Waves in Central Asia," *AN SSSR, Doklady*, Vol. 222, No. 4, 1975, pp. 829-832.

24. Ruzaikin, A. I., I. L. Nersesov, V. I. Khalturin and P. Molnar, "Propagation of Lg and Lateral Variations in Crustal Structure in Asia," *Journal of Geophysical Research*, Vol. 82, No. 2, 1977, pp. 307-316.

25. Nersesov, I. L., and T. G. Rautian, "The Study of Dynamics and Kinematics of Seismic Waves at (sic) the Profile Pamir-Baikal," Proceedings of the Eighth Assembly of the European Seismological Commission, Budapest, 1968, pp. 174-181.